J. Astrophys. Astr. (1992) **13**, 61–107

Effects of Rotation on the Colours and Line Indices of Stars 5. The ZRMS and the ZRZAMS

Annamma Mathew* & R. Rajamohan *Indian Institute of Astrophysics, Bangalore 560034*

Received 1991 August 14; accepted 1992 January 15

Abstract. The observed *uvby* and H_β indices of member stars of the Hyades and Praesepe clusters have been analysed in detail for rotation effects. The Alpha Persei, Pleiades and the Centaurus subgroup of the Scorpio—Centaurus association have been reanalysed using the observed indices instead of the extinction-corrected indices used earlier. The observed rotation effects from the analysis of these cluster data are found to be in excellent agreement with the theoretical predictions of Collins & Sonneborn (1977). We have also analysed the β, c and $(u-b)$ values of the member stars of NGC 1976, 2264, 2287, 2422, 4755, IC 2391, IC 2602 and IC 4665 for rotation effects. The results are found to be consistent with the theoretical predictions.

The observed slopes of the rotation effects were used to determine the zero rotation main sequence values of the intermediate band photometric indices for selected clusters. We also corrected the observed indices for each star in each cluster using the theoretical predictions of Collins and Sonneborn and derived the ZRMS values for each cluster. The agreement between the two determinations is found to be good. The various ZRMS curves were utilised to derive the ZRZAMS values. A preliminary calibration of the absolute visual magnitudes as a function of β valid for ZRZAMS has also been derived. The ZRMS values of the intermediate band photometric indices for different clusters and the ZRZAMS values are listed as a function of β.

Key words: stars, rotation—stars, colours—star clusters, individual

1. Introduction

The idea that axial rotation could be determined from the measurements of the widths of spectral lines was first put forward by Captain W. de Abney (1877). Since then many efforts have been made to determine the rotational velocities of various types and groups of stars (see *e.g.* reviews by Huang & Struve 1960; Slettebak 1970; Plavec 1970; Abt 1970). Simultaneously attempts were also made to estimate the changes in the structure of the stars due to rotation and the observable effects such changes would produce (see *e.g.* reviews by Roxburgh 1970; Kraft 1969; Collins 1970).

* on leave from Assumption College, Changanacherry, Kerala.

Broadly, the main results can be summarized as follows. The early type B, A and F main sequence stars rotate fairly fast while stars later than F5 are in general, very slow rotators. Amongst the early-type stars, those that are in binaries are slow rotators on an average than similar single stars, mainly due to the synchronization of rotational and orbital periods. The chemically peculiar (CP) stars of the upper main sequence are in general slow rotators. The differences between field and cluster stars and between cluster and cluster in the observed rotational velocity distribution are caused by differences in binary and CP star frequencies and by the differences in their ages. Even though there seems to be a consensus as far as these results are concerned, the situation regarding the predicted changes in the structure of these stars and their effects on the observable parameters is quite different.

In fact, the results of the analysis of observations by different authors have led to conflicting results on the possible effects of steller rotation on the observable parameters (see *e.g.* the review by Collins 1970). As of today, all existing calibrations of various parameters and the estimates of ages of stars from colour magnitude diagrams have all been done completely disregarding the (predicted) effects due to rotation.

The earliest effort in this field seems to be that of Sweet & Roy (1953) who showed that rotation modifies the luminosity of a star and that it could be as large as one magnitude relative to its non-rotating counterpart. Since then Roxburgh, Griffith & Sweet (1965) Roxburgh & Strittmatter (1965, 1966) Hardorp & Strittmatter (1968) and Collins (1963, 1965), Collins & Harrington (1966) Collins & Sonneborn (1977) and Collins & Smith (1985) have considered in detail the expected rotation effects on the various observable parameters of stars.

In general, such predicted effects in colours and the absolute magnitudes of stars and other observable parameters such as the equivalent widths of the lines are not large excepting in case of extreme rotational velocities. Attempts to verify such predicted effects were made successfully by Strittmatter (1966) in the Praesepe cluster. Strittmatter measured the difference in the observed M_v and the M_v defined by non-rotators at a fixed $(B - V)$. These deviations ΔM_v were found as expected to be proportional to $(V \sin i)^2$ based on Roxburgh & Strittmatter's (1966) work. These results, however, were questioned by Dickens, Kraft & Krzeminski (1968) who found that more accurate data do not show the expected relationship between $(U - B)$ colours and $V \sin i$.

Kraft & Wrubel (1965) attributed the large spread in c_1, $(b - y)$ diagram in Hyades to rotation effects. Strömgren (1967) pointed out that no rotation effects are discernible in the intermediate band indices while Crawford & Barnes (1974) found that the c_1 index was affected by as much as 0.035 magnitudes per $100\,\mathrm{km\,s^{-1}}$ of $V \sin i$ in A stars of α-Persei while the values of B-stars showed no such effects. Hartwick & Hesser (1974) found evidence for rotation effects in the c_1 and β indices of field A and F type stars while Rajamohan (1978) found similar evidence for B and A stars of the α-Persei cluster and the Scorpio-Centaurus association.

Similarly Guthrie (1963) found that rotation effects are indeed discernible in H_β line strengths at a given $(U - B)$ index. The theoretical predictions by Collins & Harrington (1966) are in good agreement with Guthrie's findings. However, Crawford & Manders (1966) and Petrie (1964) found no evidence for effects of rotation on H_β and H_γ line strengths respectively. Warren (1976) discussed the proposed rotation effects in some detail, for B-stars in Orion, and showed that no systematic effects are present for

$V\sin i$ less than $250\,\mathrm{km\,s^{-1}}$. Gray & Garrison (1987, 1988, 1989) from a refined MK classification of A and F type field stars, showed that indeed rotation effects can be clearly established in the intermediate band indices c_1 and β.

No consistent picture had emerged as on 1987 when we took up this work to investigate systematically the effects of rotation on the colours and line indices of stars. We decided to reinvestigate this problem in galactic clusters and determine empirically the effects of rotation on the colours and line indices of stars.

Our attempt since 1987 was to first establish that the effects of rotation on colours are not subtle but are easily discernible provided we choose a sample of single main sequence stars at the same stage of evolution. In Papers 1, 2 and 4 of this series (Rajamohan & Mathew 1988, Mathew & Rajamohan 1990a, b) it was shown that rotation effects in $uvby\ H_\beta$ and UBV colours can be firmly established for B and A stars of Alpha Persei, Pleiades clusters and the Scorpio-Centaurus association. These relative effects were basically established from the observed position of single main sequence stars in a plane defined by a combination of any two of the photometric indices. The Pleiades and Scorpio-Centaurus data were analysed using the indices corrected for interstellar extinction and the data for α-Persei cluster was analysed using the observed as well as the dereddened indices. However, Gray & Garrison (1989) pointed out that the dereddening procedures and the system calibration, especially for the A-stars are themselves affected by rotation. We, have therefore carried out our analysis of a number of clusters using the observed indices. The results which include extensive analysis of the Hyades and Praesepe are given in Section 3. In Section 4, the zero rotation main sequence (ZRMS) values of selected clusters derived are given. The results in Section 4 for various clusters are combined to derive the zero rotation zero age main sequence (ZRZAMS) values of the narrow band photometric indices and is given in Section 5. A preliminary calibration of the absolute magnitudes on the ZRZAMS is also given in this section. A summary of the results is given in the final section.

2. Data and analysis

We clarify a few details of the procedures adopted as this paper summarises the results obtained with our present approach to determine the rotation effects on intermediate band photometric indices. Each star cluster was analysed independently as the member stars are assumed to have formed coevally. This was done to avoid any zero point errors in the photometry of star clusters by different observers and to avoid systematic differences that may exist between clusters due to the differences in the distribution of their rotational velocities. All known double-lined binaries and visual binaries with Δm less than 2.0 magnitudes were excluded from analysis. Am and Ap stars that are single in general were included. However, they were found to deviate in the analysis of the $(u-b)$ index and hence were excluded from the analysis for that index.

The errors in photometry are of the order of ± 0.01 magnitudes. The errors in $V\sin i$ generally quoted are of the order of 10 per cent. However, according to Collins the errors in $V\sin i$ derived by conventional methods for stars rotating close to break-up speeds can be as large as 40 per cent. In general, such stars will be classified as *Be* and they have not been included in the analysis.

In principle it is difficult to determine rotation effects on colours as theory predicts that almost all observable parameters of the stars are affected by rotation and the magnitude of this effect depends for each star on its mass m, true rotational velocity V and i the inclination of the rotation axis to the line of sight. Thus, two objects of differing masses can have identical colour indices due to their differences in V and i (see *e.g.* Collins & Smith 1985).

Another problem is the role of interstellar extinction as both rotation and extinction lead to reddened indices. The determination of the extinction values will be uncertain especially when both effects are comparable and the individual extinction values for each star will be highly uncertain if rotation effects are not allowed for. Also as pointed out by Gray & Garrison (1989), the system calibration and dereddening procedures especially for A-stars are themselves affected by rotation which then would cast some doubt in the determination of colour excess due to extinction. Thus in order to derive the intrinsic parameters for a calibration of indices, we need to correct for extinction and rotation but the calibration procedures depend on an assumed relationship that has not taken rotation into account. Also only $V\sin i$ is observable whereas to calibrate we need to know the individual values of V and i. Also quantities such as the mass of the star, which are unaffected by rotation are unkown. Theory also predicts that rotation effects vary as a function of mass and each index varies differently (Collins & Sonneborn 1977; Collins & Smith 1985).

Our approach to this complicated problem was the following. The effect of rotation is to displace the main sequence of a cluster of coeval stars from its non-rotating counterpart and broaden it by about twice the displacement (Collins & Smith 1985). The maximum shift of a single star depends on the maximum rotational velocity that the star can rotate with; this corresponds to the balance between the centrifugal force and gravity at the equator. The distribution of the stars in the band between its zero rotation main sequence (ZRMS) and the critical velocity main sequence (CVMS) depends on the spread in the true rotational velocities of the stars. This spread is not sensitive to i. (Collins & Sonneborn 1977; Collins & Smith 1985).

Therefore one can expect, for a Maxwellian distribution in V and i, the spread to be dependent on the observed (projected) rotational velocity $V\sin i$ as only few objects will be at the tail end of such a distribution. If the spread in the distribution of V is not large as suggested by Rajamohan (1978), the observed main sequence is not expected to show a large spread caused by differences in the observed rotational velocities of the member stars. Even though the effects of the rotation of stars are nonlinear in V and $V\sin i$, such nonlinearities are important only for rotating close to their break-up speeds ($\omega = 1.0$). Only early B-stars rotate close to their break-up speeds and such objects can be generally recognised by the emission phenomenon associated with them. The maximum observed rotational velocities for others correspond to $\omega \leqslant 0.9$ (Rajamohan 1978). Hence if Be stars are excluded, then the rest of the objects can be expected to show a deviation from the ZRMS which will depend, linearly on the average observed rotational velocities of stars (Collins & Harrington 1966; Mathew & Rajamohan 1990). But the position of the ZRMS is unknown. Hence the following procedure was adopted.

We eliminated in each cluster, known Be stars, SB2's and VB's with $\Delta m < 2.0$ magnitudes. Only stars of luminosity classes IV and V were considered. In a colour-colour plot, we assume that these apparently single stars will define an average sequence parallel to the ZRMS. A single intrinsic line that defines this mean relationship also defines the average shift of the main sequence for the mean observed rotational velocities of the cluster members. The advantage of this method is that while we use all stars in a cluster to get a statistically significant sample, the intrinsic differences in the angular momentum distribution at different masses will not affect the results significantly. Errors in photometry and $V \sin i$ determinations cannot completely account for the residual scatter in all these correlation diagrams.

B and A type main sequence members were analysed separately. For each cluster, two indices were plotted against each other and a second order polynomial fit was derived. The observed minus computed $(O - C)$ residuals in each index were determined and plotted against $V \sin i$. A least square fit was derived to determine the rotation effects. The rotation effects determined are relative as both indices are affected by rotation. In general we plotted all other indices against the β index to determine the rotation effects. For selected clusters, the rotation effects were analysed in all possible planes defined by any two of the intermediate band photometric indices.

A list of clusters with available *uvby*, β and $V \sin i$ data was provided by Dr. J. Mermilliod of the University of Lausanne, Switzerland. We analysed the data of most of these clusters in which a statistically significant sample of single main sequence members with known $V \sin i$ values were present. The references to the cluster data utilised in this study are given in Table 1. A final summary of the results of all the clusters analysed is given in Table 2 and the results for all the indices for a few selected clusters are given in Tables 3, 4 and 5.

3. Results

Detailed analysis of the α-Persei cluster, the Pleiades cluster and the Scorpio-Centaurus association have already been published (Rajamohan & Mathew 1988; Mathew & Rajamohan 1990a). For the α-Persei cluster, the analysis was done using observed as well as dereddened indices. However, the other two clusters were analysed after correcting the indices of each star for interstellar extinction. There is some uncertainty in the use of dereddened indices especially for A-stars (Gray & Garrison 1989). Hence we have used observed indices in the analysis even though for clusters analysed by both procedures, the differences were only marginal. One tends to get slightly larger effects if the indices are not corrected for extinction especially in the $(u - b)$ index for B stars.

The slopes of the rotation effects determined in the (β, c) plane and the $(\beta, u - b)$ plane for all the clusters studied are given in Table 2. The symbol Δ is used to denote the residual in a given index in a given plane. For example, in the (β, c) plane, $\Delta\beta$ is defined as the difference between β observed and the calculated β value for its observed c value. Similarly, Δc is defined as the difference between c observed and the calculated c value for its observed β. The calculated values were determined from a second-order polynomial fit to the observed values of β and c.

As in Paper 2 (Mathew & Rajamohan 1990a), the slopes of rotation effects were derived from the theoretical predictions of Collins & Sonneborn (1977). In order to compare the predictions from theoretical models of Collins & Sonneborn (1977), we have analysed the theoretical u, v, b, y and H_β indices in a similar way as we did for the cluster data. For this we have arranged the stars into three groups: B0 to B3, B5 to B9 and A3 to F0. For each group at a given value of i and different values of ω, a second-order polynomial fit was determined for each of the various pairs of colour indices like β versus c_1, β versus $(u-b)$ *etc* and the deviations $\Delta\beta$, Δc, $\Delta\ (u-b)$, $\Delta(b-y)$ etc were determined. This was done for $i = 30°, 45°, 60°$ and $90°$. The slopes of the relation between $V \sin i$ and the colour excess derived for different values of i are given in Tables 3–5 along with the observed rotation effects in α-Persei, Pleiades, Hyades, Praesepe and the members of the lower and upper Centaurus subgroup of the Scorpio-Centaurus association. The choice of this subgroup is given as an example

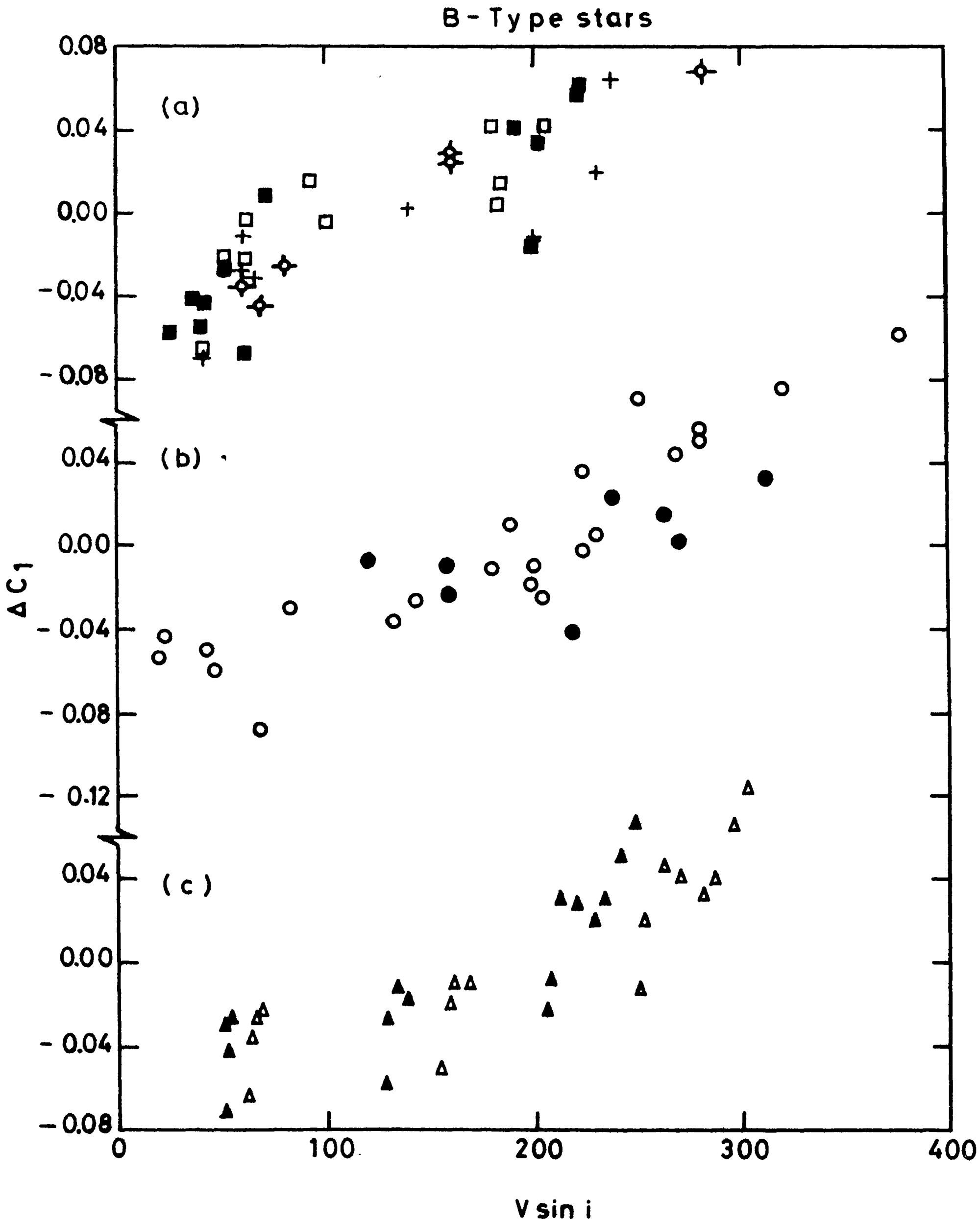

Figure 1. Residuals in c_1, derived from the observed mean relationship in the (β, c_1) plane for B-stars are plotted against $V \sin i$ for (a) IC 2391 (squares), IC 4665 (filled squares), NGC 2264 (circles with cross bars) and NGC 2422 (plus); (b) Pleiades (filled circles) and α-Persei (open circles); (c) Residuals derived from theoretical predictions by Collins & Sonneborn (1977) for B5–B9 stars for $i = 45°$ (filled triangles) and $i = 60°$ (open triangles) are shown for comparison.

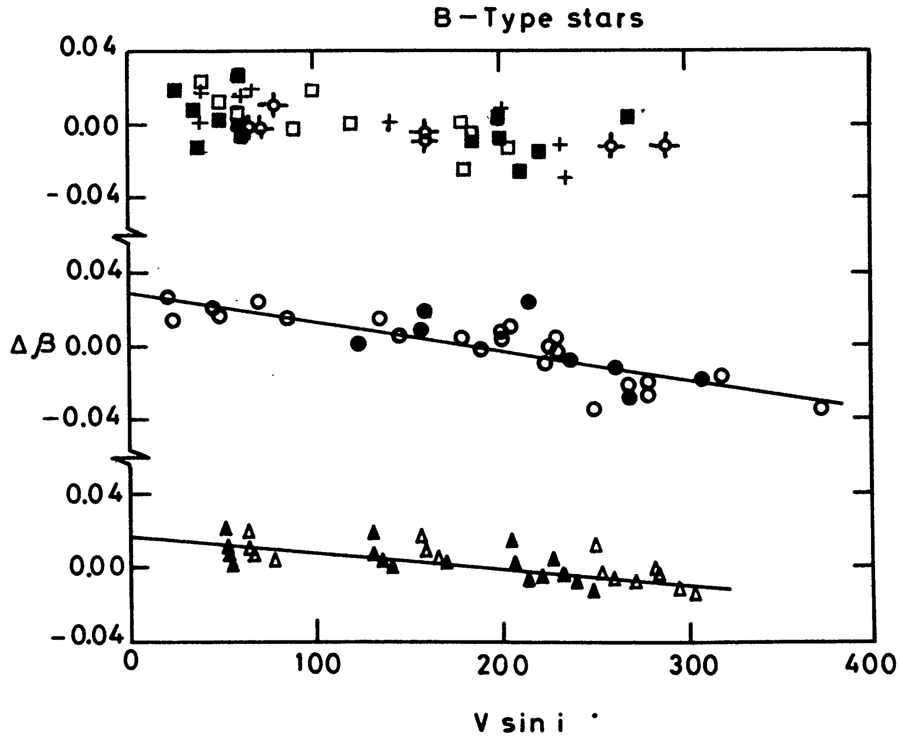

Figure 2. The residuals $\Delta\beta$ derived for B-stars from the (β, c) relationship is plotted against $V \sin i$. Symbols have the same meaning as in Fig. 1.

as it represents a least reddened sample of pure B2 and B3 main sequence stars. The B5 to B9 range is represented by the α-Persei B-stars while Hyades and Praesepe represent the A3-F2 type domain. The A3 to F2 domain is also represented by the α-Persei and Pleiades clusters.

These results for the B-stars are shown in Figs 1–3. In Figs 1 and 2 the residuals in c_1 and β derived from the (β, c) relationship are plotted against $V \sin i$. The results for the B-stars in α-Persei, Pleiades, IC 2391, IC 4665, NGC 2264 and NGC 2422 have been plotted. We have shown for comparison the theoretically expected relationship for the B5-B9 mass range derived from the calculations of Collins & Sonneborn (1977) for representative i value of 45° and 60°.

Fig. 3 is similar to Fig. 1. The residuals in $(u-b)$ derived from the $(\beta, u-b)$ relationship have been plotted. The $(b-y)$ results derived from the $(\beta, b-y)$ plane are shown in Fig 4.

Results for the A-stars are shown in Figs 5–9. The deviations in c_1 and β derived from the (β, c) plane have been plotted against $V \sin i$ for α-Persei, Pleiades, IC 4665, IC 4756, NGC 2516, Coma, Hyades and Praesepe in Figs 5 and 6. The results from the theoretical predictions for the A3-F2 mass range are also shown for comparison. Similarly $\Delta(u-b)$ from $(\beta, u-b)$ relation, $\Delta(b-y)$ from $(c_1, b-y)$ relation and Δm_1 from (c_1, m_1) relation have been plotted against $V \sin i$ in Figs 7–9 respectively.

It can be easily noticed from Tables 2–5 and Figs 1–9 that the observations are in excellent agreement with the theoretical predictions of Collins & Sonneborn (1977).

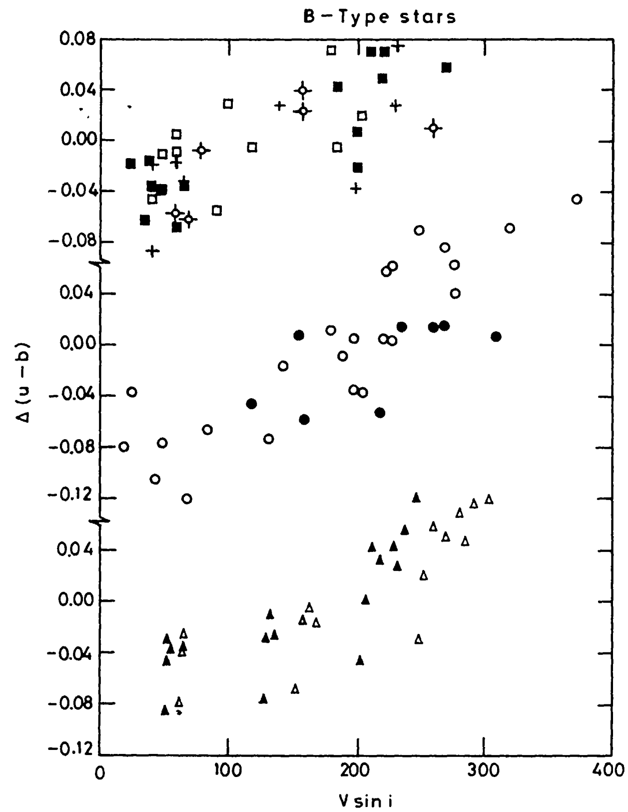

Figure 3. Δ $(u-b)$ versus $V\sin i$ derived for B-stars from the $(\beta, u-b)$ relation. Symbols have same meaning as in Fig. 1.

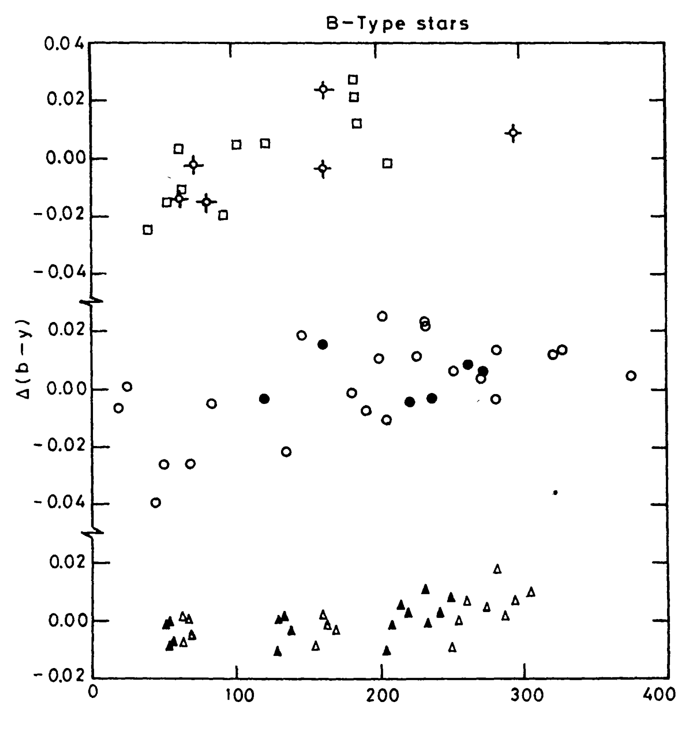

Figure 4. The residuals Δ $(b-y)$ for B-stars from the $(\beta, b-y)$ relation is plotted against $V\sin i$. Symbols have the same meaning as in Fig. 1.

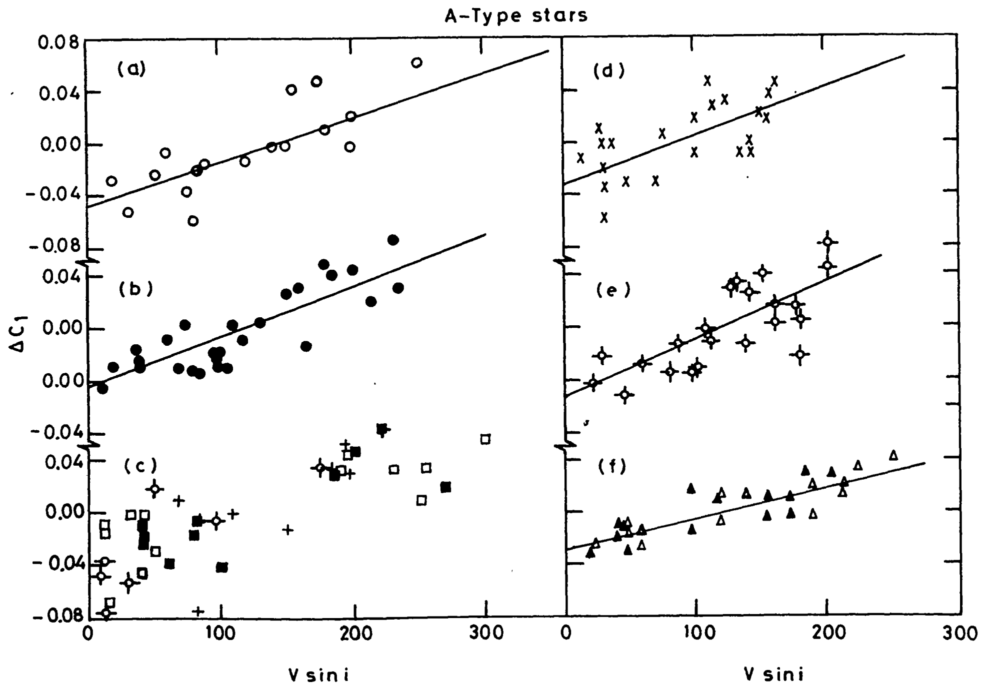

Figure 5. Δc_1 versus $V\sin i$ diagram derived from the (β, c_1) plane for A stars in various clusters (a) ○ α-Persei (b) ● Pleiades (c) ■ IC 4665. -✧- Coma, + IC 4756, □ NGC 2516 (d) × Hyades (e) -✧- Praesepe (f) ▲ $i = 45°$ and △ $i = 60°$ derived from theoretical predictions.

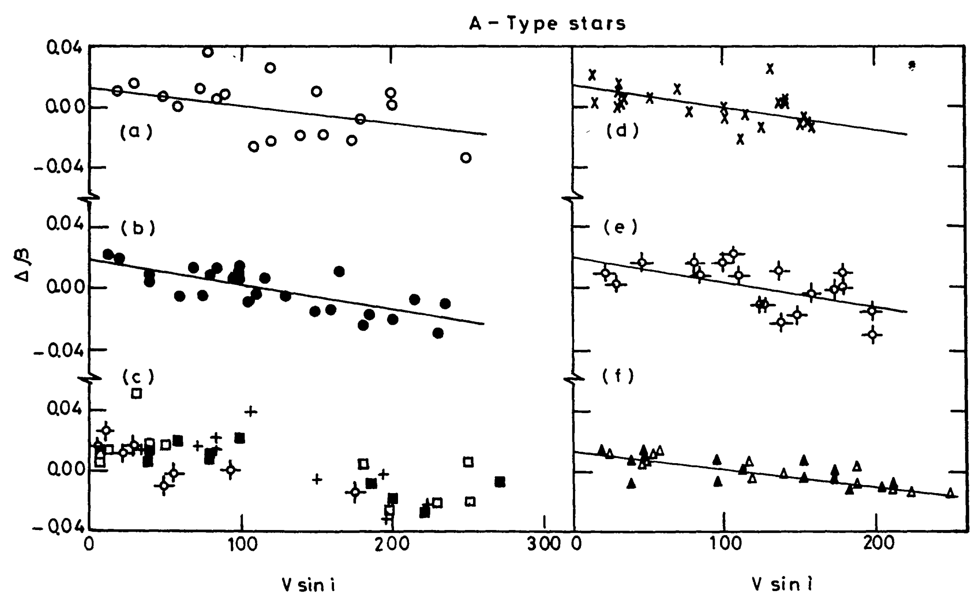

Figure 6. The $\Delta\beta$ versus $V\sin i$ diagram derived from (β, c_1) plane for A-stars in various clusters. Symbols have the same meaning as in Fig. 5.

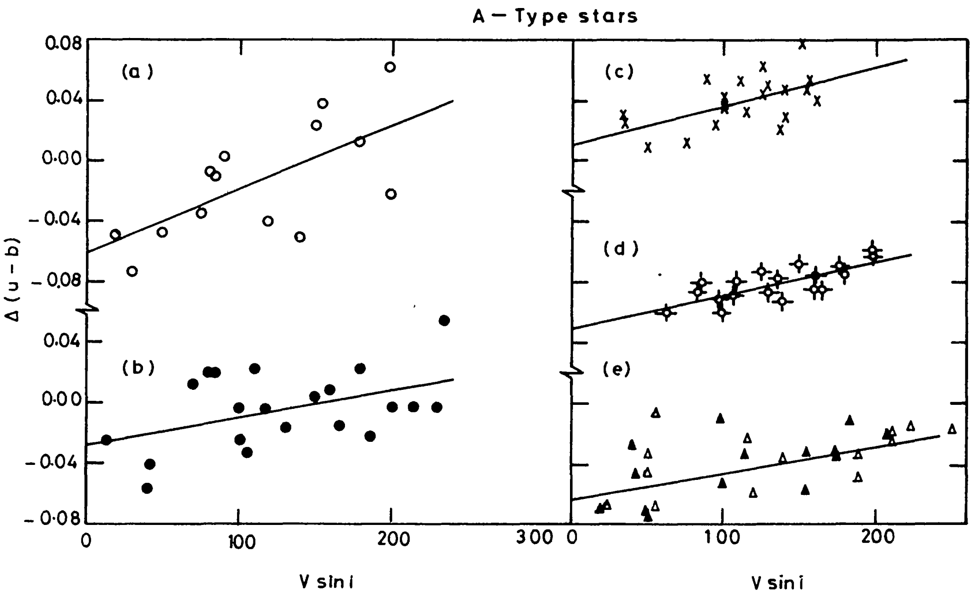

Figure 7. Δ $(u-b)$ $V\sin i$ diagram derived from the $(\beta,\ u-b)$ relationship for (a) α-Persei (b) Pleiades (c) Hyades (d) Praesepe and (e) theoretical predictions for $i = 45°$ and $i = 60°$.

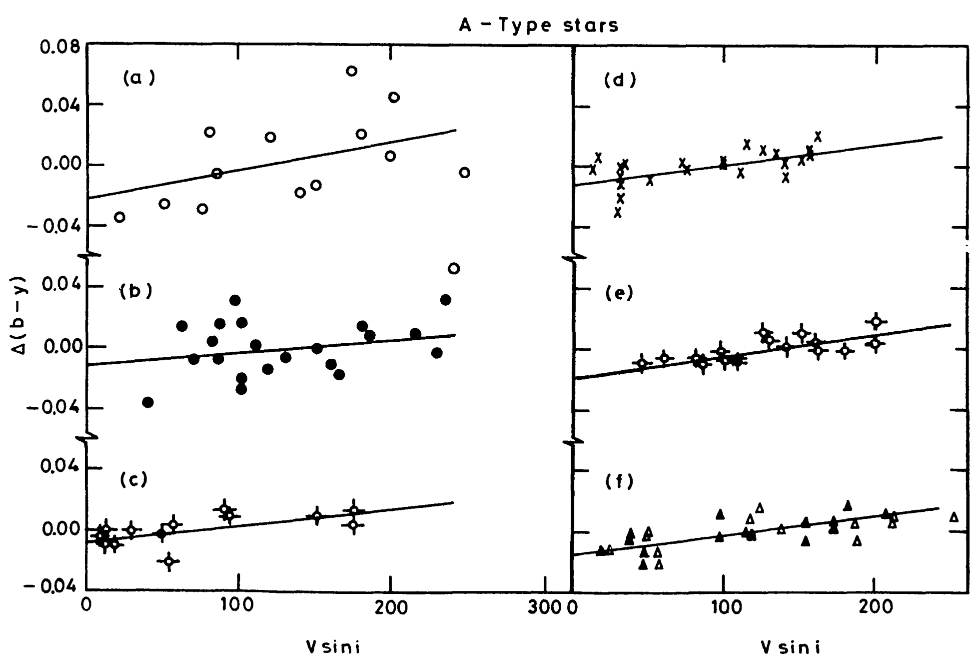

Figure 8. Δ $(b-y)$ versus $V\sin i$ diagram from $(c_1, b-y)$ plane for A stars in various clusters. Symbols have the same meaning as in Fig. 5.

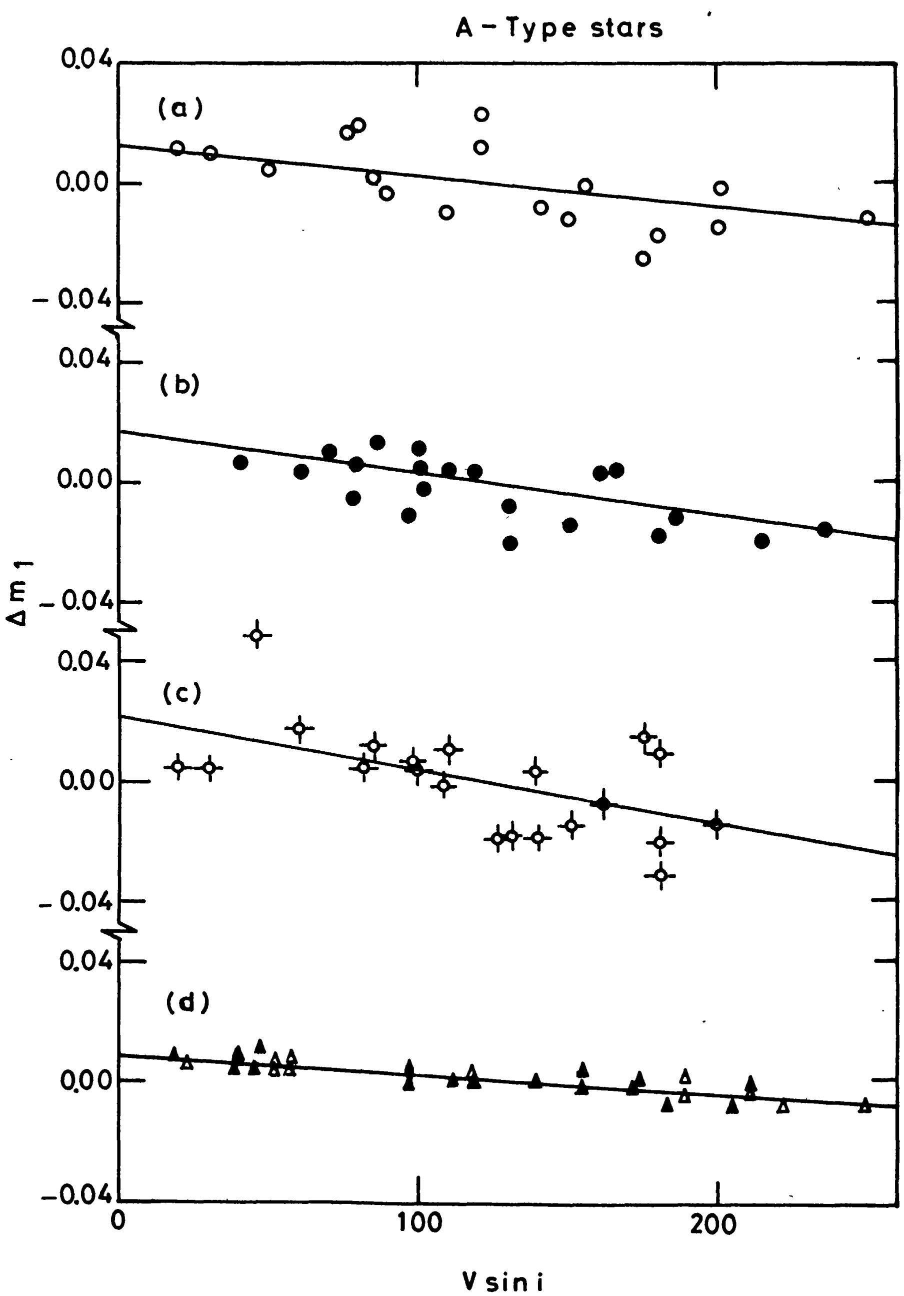

Figure 9. Δm_1 versus $V\sin i$ diagram derived from the (c_1, m_1) relationship for (a) α Persei (b) Pleiades (c) Praesepe and (d) theoretical predictions for $i = 45°$ and $60°$.

Table 1. References to cluster data.

Cluster	Data	Reference	Cluster	Data	Reference
α-Persei (mel 020)	$uvby\ H_\beta$	Crawford & Barnes (1974)	Coma	$uvby\ H_\beta$	Crawford & Barnes (1969)
	UBV	Mitchell (1960)		UBV	Johnson & Kunckles (1955)
	$V \sin i$	Kraft (1967)		$V \sin i$	Kraft (1965)
	ST	Morgan Hiltner & Garrison (1971)		ST	Mendoza (1963)
Pleiades (mel 022)	$uvby H_\beta$	Crawford & Perry (1976)	Cep OB3	$uvby H_\beta$	Crawford & Barnes (1970)
	UBV	Johnson & Mitchell (1958)		UBV	Blaauw, Hiltner & Johnson (1959)
	$V \sin i$	Anderson, Stoeckly & Kraft (1966)		$V \sin i$	Garmany (1973)
	ST	Mendoza (1956)			
Hyades (mel 025)	$uvby H_\beta$	Crawford & Perry (1966)	NGC 1039	$uvby H_\beta$	Canterna & Perry (1979)
	UBV	Johnson & Knuckles (1955)		$V \sin i$	Ianna (1970)
	$V \sin i$	Kraft (1965)		ST	Ianna (1970) Abt & Levato (1977)
	ST	Morgan & Hiltner (1965)			
Praesepe (NGC 2632)	$uvby H_\beta$	Crawford & Barnes (1969)	NGC 1976	$uvby H_\beta$	Warren & Hesser (1977)
	UBV	Johnson (1952)		$V \sin i$	Abt, Muncaster & Thompson (1970) Mc Namara & Larson (1961)
	$V \sin i$	Mc Gee, Khogali, Baum & Kraft (1967)			
	ST	Bidelman (1956)		ST	Abt & Levato (1977)
Sco-Cen	$uvby H_\beta$	Glaspey (1971)	NGC 2264	$uvby H_\beta$	Strom, Strom & Yost (1971)
	UBV	Moreno & Moreno (1968)		$V \sin i$	Vogel & Kuhi (1981)
	$V \sin i$	Rajamohan (1976) Slettebak (1968) Uesugi & Fukuda (1982)		ST	Yong (1978)
	ST	Garrison (1967)			
NGC 2287	$uvby H_\beta$	Nissen (1988) Eggen (1974, 1981)	IC 2391	$uvby H_\beta$	Perry & Hill (1969)
	$V \sin i$	Levato & Garcia (1984)		$V \sin i$	Levato (1974)
	ST	Hartoog (1976)		ST	Perry & Bond (1969)
NGC 2422	$uvby H_\beta$	Shobbrook (1984)	IC 2602	$uvby H_\beta$	Hill & Perry (1969)
	UBV	Hoag *et al* (1961) Smyth & Nandy (1962)		UBV	Braes (1962)
	$V \sin i$	Dworetsky (1975)		$V \sin i$	Levato (1975)
NGC 2516	$uvby H_\beta$	Snowden (1975)	IC 4665	$uvby H_\beta$	Crawford & Barnes (1972)
	$V \sin i$	Abt & Clements (1969)		UBV	Hogg & Kron (1955)
	ST	Abt & Morgan (1969) Hartoog (1976)		$V \sin i$	Abt & Chaffee (1967)

Table 1. Continued

Cluster	Data	Reference	Cluster	Data	Reference
NGC 4755	$uvbyH_\beta$	Shobbrook (1984)	IC 4756	$uvbyH_\beta$	Schmidt (1978)
	UBV	Perry, Franklin, Landolt & Crawford (1976)		$V\sin i$	Schmidt & Forbes (1984)
	$V\sin i$	Balona (1975)		ST	Herzog, Sanders & Seggewiss (1975)
	ST	Feast (1963) Schild (1970)			
NGC 6475	$uvbyH_\beta$	Snowden (1976)			
	$V\sin i$	Abt & Jewsbury (1969)			

Table 2. Observed reddening due to rotation for $100\,\mathrm{km\,s^{-1}}$ of $V\sin i$.

	from (β, c_1)		from ($\beta, u-b$)	
Cluster	$\Delta\beta$	Δc_1	$\Delta\beta$	$\Delta(u-b)$
Hyades	−.015 ±.002	.037 ±.006	−.022 ±.005	.026 ±.006
Praesepe	−.015 ±.003	.037 ±.006	−.028 ±.004	.022 ±.004
Pleiades A stars	−.017 ±.002	.039 ±.004	−.015 ±.007	.018 ±.006
α-Persei A stars	−.014 ±.004	.030 ±.006	.012 ± 006	.043 ±.008
α-Persei B stars	−.015 ±.001	.045 ±.003	−.013 ±.001	.062 ±.005
IC 4665 A stars	−.016 ±.003	.033 ±.006		
IC 4665 B stars	−.013 ±.002	.043 ±.007	−.010 ±.002	.045 ±.005
NGC 2264	−.008 ±.001	.038 ±.006	−.007 ±.001	.052 ±.001
IC 2391	−.016 ±.003	.038 ±.007	−.019 ±003	.066 ±016
IC 2602	−.013 ±.004	.036 ±.011	−.012 ±.004	.057 ±.015
NGC 2422	−.013 ±.003	.032 ±.008	−.013 ±.004	.036 ±.011
NGC 4755	−.011 ±.002	.032 ±.005	−.008 ±.002	.031 ±.007
Scorpio-Centaurus	−.007 ±.001	.028 ±.003	−.006 ±.001	.033 ±.004
NGC 2287	−.006 ±.004	.020 ±.024	−.026 ±.007	.064 ±.016
NGC 1976	−.007 ±.003	.032 ±.011	−.002 ±.002	.013 ±.011

Table 3. Theoretical reddening due to rotation for 100 km s^{-1} of $V \sin i$ for B0 to B3 stars.

	from (β, c_1)		from $(\beta, b-y)$		from $(\beta, u-b)$		from (β, m_1)		from $(c_1, b-y)$	
i	$\Delta\beta$	Δc_1	$\Delta\beta$	$\Delta(b-y)$	$\Delta\beta$	$\Delta(u-b)$	$\Delta\beta$	Δm_1	Δc_1	$\Delta(b-y)$
30	−.004 ±.000	.021 ±.002	−.004 ±.000	.004 ±.000	−.004 ±.000	.027 ±.003	.003 ±.001	−.001 ±.000	−.001 ±.001	.001 ±.000
45	−.003 ±.000	.016 ±.002	−.004 ±.000	.003 ±.000	−.003 ±.000	.022 ±.003	.002 ±.001	−.001 ±.000	−.004 ±.001	.001 ±.000
60	−.003 ±.000	.016 ±.002	−.004 ±.000	.003 ±.000	−.003 ±.000	.021 ±.002	.001 ±.000	.000 ±.000	−.003 ±.001	.001 ±.000
90	−.003 ±.000	.015 ±.002	−.003 ±.000	.003 ±.000	−.003 ±.000	.021 ±.002	.001 ±.000	−.000 ±.000	−.002 ±.001	.001 ±.000
	Observed reddening due to rotation for 100 km s^{-1} of $v \sin i$ for B0, B3 stars.									
Upper-Cen + Lower-Cen B2, B3 stars	−.005 ±.002	.017 ±.006	−.004 ±.003	.000 ±.002	−.006 ±.001	.028 ±.006	−.002 ±.003	.001 ±.001	−.002 ±.009	−.001 ±.001

Theoretical reddening due to rotation for 100 km s^{-1} of $V \sin i$ for B0, B3 stars.

	from $(c_1, u-b)$		from (c_1, m_1)		from $(b-y, u-b)$		from $(b-y, m_1)$		from $(u-b, m_1)$	
i	Δc_1	$\Delta(u-b)$	Δc_1	Δm_1	$\Delta(b-y)$	$\Delta(u-b)$	$\Delta(b-y)$	Δm_1	$\Delta(u-b)$	Δm_1
30	.001	−.001	.038	−.001	.001	−.004	.006	−.001	.050	−.001
	±.000	±.001	±.005	±.000	±.000	±.001	±.001	±.000	±.007	±.000
45	.001	−.001	.028	−.001	.001	−.004	.005	−.001	.038	−.001
	±.000	±.001	±.003	±.000	±.000	±.001	±.001	±.000	±.004	±.000
60	.000	.000	.020	.001	.001	−.004	.004	−.001	.027	−.001
	±.000	±.000	±.003	±.000	±.000	±.001	±.001	±.000	±.004	±.000
90	.000	.000	.018	−.001	.001	−.004	.003	−.001	.025	−.001
	±.000	±.000	±.003	±.000	±.000	±.000	±.000	±.001	±.004	±.000
	Observed reddening due to rotation for 100 km s^{-1} of $V \sin i$ for B2, B3 stars.									
Upper-Cen	.000	−.000	.010	−.001	−.002	−.001	−.002	.000	.006	−.001
Lower-Cen	±.003	±.004	±.013	±.001	±.001	±.011	±.003	±.002	±.017	±.001
B2, B3 stars										

Table 4. Theoretical reddening due to rotation for 100 km s^{-1} of $V \sin i$ for B5 to B9 stars.

	from (β, c_1)		from ($\beta, b-y$)		from ($\beta, u-b$)		from (β, m_1)		from ($c_1, b-y$)	
i	$\Delta\beta$	Δc_1	$\Delta\beta$	$\Delta(b-y)$	$\Delta\beta$	$\Delta(u-b)$	$\Delta\beta$	Δm_1	Δc_1	$\Delta(b-y)$
30	−.014 ±.002	.058 ±.007	−.010 ±.003	.006 ±.002	−.012 ±.002	.066 ±.009	.007 ±.001	−.001 ±.000	.006 ±.005	.000 ±.002
45	−.011 ±.001	.046 ±.005	−.009 ±.002	.005 ±.001	−.010 ±.002	.054 ±.007	.006 ±.001	−.001 ±.000	.000 ±.004	.000 ±.001
60	−.010 ±.001	.041 ±.004	−.008 ±.002	.005 ±.001	−.009 ±.001	.049 ±.006	.005 ±.001	−.001 ±.000	.001 ±.003	.000 ±.001
90	−.009 ±.001	.038 ±.004	−.007 ±.002	.005 ±.001	−.008 ±.001	.047 ±.005	.002 ±.000	−.000 ±.000	.000 ±.003	.000 ±.001

Observed reddening due to rotation for 100 km s^{-1} of $V \sin i$ for α-Persei B stars.

	$\Delta\beta$	Δc_1	$\Delta\beta$	$\Delta(b-y)$	$\Delta\beta$	$\Delta(u-b)$	$\Delta\beta$	Δm_1	Δc_1	$\Delta(b-y)$
α-Persei B stars	−.015 ±.001	.045 ±.003	−.017 ±.005	.010 ±.002	−.013 ±.001	.062 ±.005	.007 ±.005	−.002 ±.002	−.013 ±.015	.002 ±.002

Theoretical reddening due to rotation for 100 km s^{-1} of $V \sin i$ for B5 and B9 stars.

	from $(c_1, u-b)$		from (c_1, m_1)		from $(b-y, u-b)$		from $(b-y, m_1)$		from $(u-b, m_1)$	
i	Δc_1	$\Delta(u-b)$	Δc_1	Δm_1	$\Delta(b-y)$	$\Delta(u-b)$	$\Delta(b-y)$	Δm_1	$\Delta(u-b)$	Δm_1
30	.007	−.009	.087	−.004	.000	−.010	.009	−.004	.106	−.004
	±.002	±.003	±.009	±.001	±.001	±.006	±.002	±.001	±.013	±.001
45	.005	−.006	.070	−.003	.001	−.006	.008	−.003	.085	−.003
	±.002	±.003	±.006	±.001	±.001	±.005	±.001	±.001	±.008	±.001
60	.003	−.004	.050	−.002	.000	−.004	.005	−002	.060	−·002
	±.001	±.002	±.006	±.000	±.001	±.004	±.001	±.001	±.008	±.000
90	.003	−.004	.047	−.002	.000	−.004	.005	−.002	.057	−.002
	±.001	±.002	±.005	±.000	±.000	±.003	±.001	±.001	±.007	±.000
	Observed reddening due to rotation for 100 km s^{-1} of $V \sin i$ for B stars.									
α-Persei	.005	−.009	.072	−.007	.003	−.024	.012	−.006	.096	−.006
B stars	+.002	±.004	±.015	±.001	±.002	±.019	±.004	±.002	±.022	±.001

Table 5. Theoretical reddening due to rotation for 100 km s^{-1} of $V \sin i$ for A3 to F0 stars.

	from (β, c_1)		from ($\beta, b-y$)		from ($\beta, u-b$)		from (β, m_1)		from ($c_1, b-y$)	
i	$\Delta\beta$	Δc_1	$\Delta\beta$	$\Delta(b-y)$	$\Delta\beta$	$\Delta(u-b)$	$\Delta\beta$	Δm_1	Δc_1	$\Delta(b-y)$
30	−016 ±.002	.035 ±.004	.003 ±.002	.003 ±.002	−.003 ±.007	.033 ±.006	.009 ±.002	−.004 ±.001	.041 ±.006	.020 ±.003
45	−.012 ±.001	.027 ±.003	.000 ±.001	.000 ±.001	−.022 ±.005	.022 ±.005	.005 ±.001	−.002 ±.000	.026 ±.005	.013 ±.002
60	−.011 ±.001	.022 ±.003	−.002 ±.001	−.001 ±.001	−.018 ±.004	.017 ±.004	.003 ±.001	−.001 ±.000	.019 ±.004	.009 ±.002
90	−.008 ±.001	.016 ±.003	−.002 ±.001	−.002 ±.001	−.011 ±.004	.010 ±.003	.002 ±.001	−.001 ±.000	.012 ±.003	.006 ±.002
	Observed reddening due to rotation for 100 km s^{-1} of $V \sin i$ for A-type stars.									
α-Persei	−.014 ±.004	.030 ±.006	−.013 ±.005	.007 ±.005	.012 ±.014	.043 ±.008	.068 ±.006	−.016 ±.002	.065 ±.012	.019 ±.006
Pleiades	−.017 ±.002	.039 ±.004	−.012 ±.004	−.013 ±.004	−.015 ±.007	.018 ±.006	.041 ±.002	−.011 ±.002	.023 ±.010	.008 ±.005
Hyades	−.015 ±.002	.037 ±.006	−.004 ±.003	−.003 ±.003	−.022 ±.005	.026 ±.006	.003 ±.003	−.002 ±.002	.028 ±.006	.013 ±.003
Praesepe	−.015 ±.003	.037 ±.006	−.018 ±.002	−.017 ±.002	−.028 ±.004	.022 ±.004	.003 ±.003	−.004 ±.002	.035 ±.005	.015 ±.002

Table 5. Continued.

	from $(c_1, u-b)$		from (c_1, m_1)		from $(b-y, u-b)$		from $(b-y, m_1)$		from $(u-b, m_1)$	
i	Δc_1	$\Delta(u-b)$	Δc_1	Δm_1	$\Delta(b-y)$	$\Delta(u-b)$	$\Delta(b-y)$	Δm_1	$\Delta(u-b)$	Δm_1
30	−.038	.017	.055	−.011	.036	.035	−.006	−.003	.042	−.018
	±.013	±.005	±.007	±.001	±.009	±.007	±.003	±.001	±.007	±.003
45	−.021	.010	.037	−.008	.022	.021	−.005	−.002	.027	−.012
	±.009	±.004	±.005	±.001	±.007	±.005	±.002	±.001	±.005	±.002
60	−.015	.007	.028	−.006	.017	.015	−.004	−.002	.020	−.009
	±.007	±.003	±.004	±.001	±.005	±.004	±.002	±.001	±.004	±.002
90	−.007	.003	.021	−.005	.010	.008	−.004	−.002	.012	−.006
	±.007	±.003	±.004	±.001	±.005	±.004	±.002	±.001	±.004	±.002
	Observed reddening due to rotation for 100 km s^{-1} for A-type stars.									
α-Persei	.038	.018	.145	−.010	−.013	.050	−.040	−.007	.065	−.006
	±.020	±.009	±.016	±.003	±.012	±.012	±.007	±.002	±.013	±.003
Pleiades	.059	−.014	.125	−.014	−.021	−.004	−.048	−.013	.029	−.008
	±.018	±.009	±.011	±.002	±.012	±.011	±.005	±.002	±.010	±.003
Hyades	.021	−.009	.017	−.007	−.016	−.029	.004	−.025	.021	−.014
	±.041	±.005	±.025	±.003	±.006	±.008	±.013	±.003	±.007	±.003
Praesepe	.066	−.030	.025	−.013	−.016	.000	−.011	−.016	−.002	−.003
	±.014	±.006	±.023	±.003	±.005	±.005	±.008	±.004	±.008	±.003

4. Zero rotation main sequence (ZRMS) of selected star clusters

As the distance scale of the Universe is literally based on the observations of the nearby Hyades cluster, we first discuss the determination of the Hyades ZRMS. The observed colour indices are of course free of interstellar extinction for this cluster. We took two approaches to the determination of ZRMS values for each clusters.

4.1 *ZRMS from Observed Slopes of Rotation Effects*

In this approach, the observed rotation effects in different planes listed in Tables 2–5 were utilised to derive the ZRMS values as a function of β. This table does not reflect the true effects due to rotation as the slopes determined are relative. In these determinations two photometric quantities, say X versus Y are plotted and a polynomial fit is derived. The residuals ΔX in X at the observed value of Y and ΔY in Y at the observed value of X are plotted against $V \sin i$ to determine the rotation effects. The observed effects are therefore relative and the true effects cannot be determined unless one of the quantities X or Y is independent of rotation, such as the mass of the star.

However, we can use the slope of the relationship between ΔX and $V \sin i$ or ΔY and $V \sin i$ to determine where the non-rotating sequence actually lies. This can be done by shifting the obseved points either in X or Y by an amount corresponding to its observed $V \sin i$ value. Even though the shifted value for each star does not correspond to the appropriate ZRMS value for its mass, the locus of the shifted positions of all stars would define the ZRMS in that plane. This method should work as long as the relationship between X and Y is not highly nonlinear and also that ΔX and ΔY are not highly nonlinear with $V \sin i$. The analysis of B and A stars independently should partially take care of such nonlinearity in the relationship between different quantities. Also for ω up to 0.9 ($V \leqslant 250\,\mathrm{km\,s^{-1}}$), the residuals can be expected to be linear (see Fig. 17 of Collins & Harrington 1966 and Fig. 5 of Collins & Smith 1985).

This was the logic followed for deriving the ZRMS values of different indices for each cluster from observationally determined slopes.

4.2 *ZRMS from Theoretical Predictions*

As the analysis of observations are in excellent agreement with theoretical predictions of Collins & Sonneborn (1977) one can in principle utilize the predicted effects to correct the observed data for each star to derive its ZRMS value. However, the value of i, the inclination between the rotation axis and the line of sight remains unknown. But we can derive the average ZRMS curve statistically based on the assumption that i is close to 60°.

Collins & Sonneborn (1977) list the effects as a function of mass for various values of V and i. They have also given the other indices like $(b-y)_0$ *etc.* as a function of mass. Collins & Smith (1985) have also listed the Zero Rotation Zero Age values as a function of mass for the A-stars. As the values in the latter paper appear to be more consistent with observations, we have combined the two tables appropriately to derive the theoretical values of $(b-y)_0$, m_0 and c_0 as a function of mass.

The calculations of rotation effects by Collins & Sonneborn (1977) for the mass range $14.5\,M_\odot$ to $1.5\,M_\odot$ for $\omega = 0.2$ and $\omega = 0.9$ and $i = 60°$ were used to produce a table of average corrections in β, c_1, $(b-y)$, $(u-b)$ and m_1 for $100\,\mathrm{km\,s^{-1}}$ of $V \sin i$. This is given in Table 6. The results from Collins & Smith (1985) were appropriately combined with those of Collins & Sonneborn (1977) to get the corresponding values of $(b-y)_0$ *etc* for the entire mass range. The table for rotation corrections in different indices were listed as a function of $(b-y)_0$ as the masses of stars are unknown. For A-stars the observed $(b-y)_0$ value was used to get the first set of corrections in $(b-y)$, $(c_1, u-b)$, m_1 and β. The corrected $(b-y)$ was used to derive a second set of corrections in $(b-y)$, c_1 *etc*. The average of these two sets was used to correct each and every star for its observed value of $V \sin i$. For B-stars, we followed the same procedure using the observed $(u-b)_0$ index instead of the $(b-y)_0$ index.

4.3 *ZRMS of Hyades*

4.3.1 *ZRMS values of β and c_1*

The observed rotation effects listed in Table 5 were used to correct, β and c_1 in the (β, c_1) plane. We denote these corrected indices as β_{ZR} and c_{1ZR} respectively.

As mentioned in the previous section we plot β_{ZR} versus c_1 and c_{1ZR} versus β. The locus of these two plots should coincide. These are shown in Fig. 10(a). A least-square fit to the data points in the figure was derived to detemine the (β_{ZR}, c_{1ZR}) relationship for Hyades. We list these ZRMS values (at equal intervals of β) in Table 7. β is chosen as an independent parameter following Crawford as it is free of instersteller extinction. The range in β for which the ZRMS values are listed corresponds to the observed range of β in Hyades.

Similarly, following Method 1b, we use the theoretical corrections listed in Table 6 to correct the individual stars in β and c_0. The corrected position and the least-square fit to the data points are shown in Fig. 10(b). The derived ZRMS values are given separately in Table 7.

The observed values of β and c_1 for all stars together with the ZRMS given in Table 7 are shown in Fig. 10(c). The Am stars are shown as filled circles, the apparent normal single stars are plotted as open circles and the SB2's and VB's with $\Delta m < 2.0$ mag as crosses.

4.3.2 *ZRMS values of $(b-y)$*

From Tables 4 and 5 we see that in the $(\beta, b-y)$ plane, rotation effects are negligible, while in the $(c_1, b-y)$ plane they are discernible. The first set of $(b-y)_{ZR}$ values was derived from a least-square fit between β and $(b-y)$. A second set was derived by correcting for rotation effects in the $(c_1, b-y)$ plane following procedures already described in the case of β, c_1. Now the $(b-y)_{ZR}$ values that correspond to β_{ZR} and c_{ZR} listed in Columns 1 and 4 of Table 7 were calculated. The $(b-y)_{ZR}$ values from both these methods were found to agree very well. The average of the two values is listed in Column 2 of Table 7.

The same values derived by using Method 1b are listed in Column 7 of Table 7. The observed positions of stars together with the ZRMS derived from observed slopes in the $(\beta, b-y)$ plane are shown in Fig 11(a).

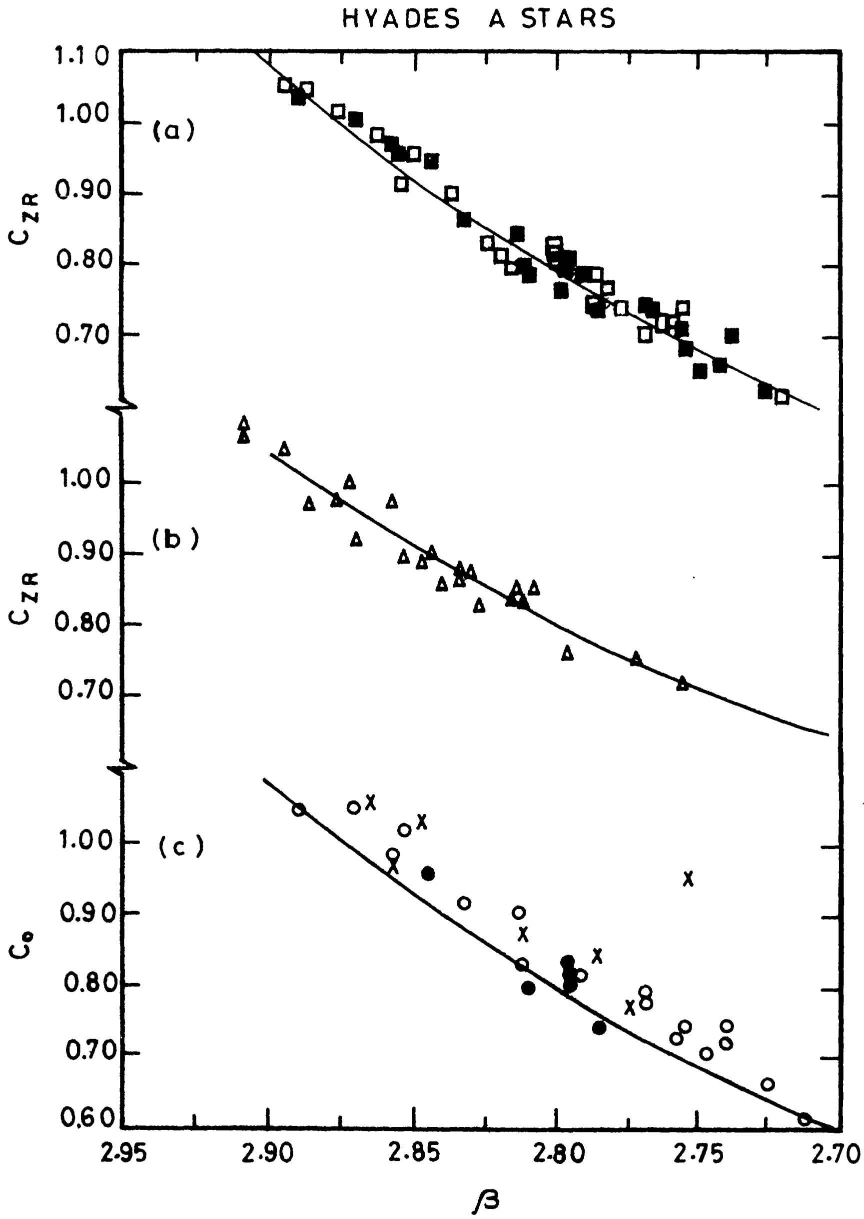

Figure 10. The ZRMS of Hyades cluster in the spectral type range A3–F0.
(a) Corrected positions of stars in the (c_1, β) plane. Each star has been plotted twice; the observed c_1 value versus β corrected for rotation effect and the c_1 value corrected for rotation versus the observed β value have been plotted. The locus defined by the least-square fit to the data points which defines the zero rotation values from observed slopes of rotation effects is shown by a continuous line. (b) The c_0 and β index independently corrected for rotation effects for each star is shown. The least-square fit is shown by the continuous line which defines the zero rotation values determined from theoretically derived slopes for $i = 60°$ from the work of Collins & Sonneborn (1977). (c) The observed position of all stars have been plotted in the c_0, β plane. The continuous line is the ZRMS determined from (a).

4.3.3 *ZRMS values of* $(u - b)$

Following procedures set up for c_1 and $(b - y)$, the $(u - b)_{ZR}$ values derived from observed effects (Method 1a) are listed in Column 5 of Table 7 and those derived from theoretical expectations (Method 1b) are listed in Column 10 of Table 7.

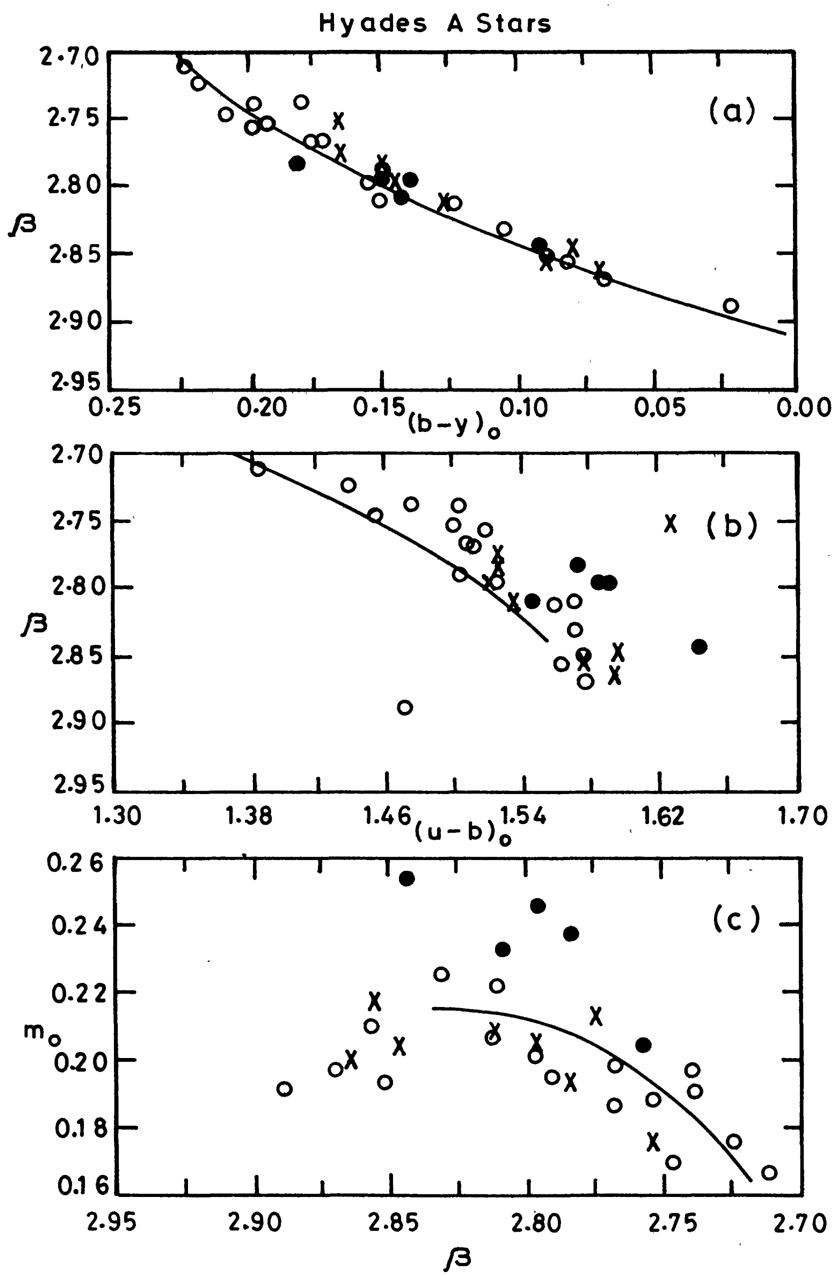

Figure 11. Same as Fig. 10 (a) The observed $(\beta, b-y)$ values of Hyades stars are plotted. The ZRMS locus determined from observed slopes of rotation effects is shown as a continuous line. (b) & (c): Same as (a) in the $(\beta, u-b)$ and β, m_1 planes.

The $(\beta, u-b)$ ZRMS curve together with the observed $(\beta, u-b)$ values of the Hyades members is shown in Fig. 11(b).

4.3.4 *ZRMS values of* m_1

The ZRMS values of m_1 were calculated from the observed rotation effects in the (β, m_1) plane and (c_1, m_1) plane. The average value of m_{1ZR} thus derived was compared

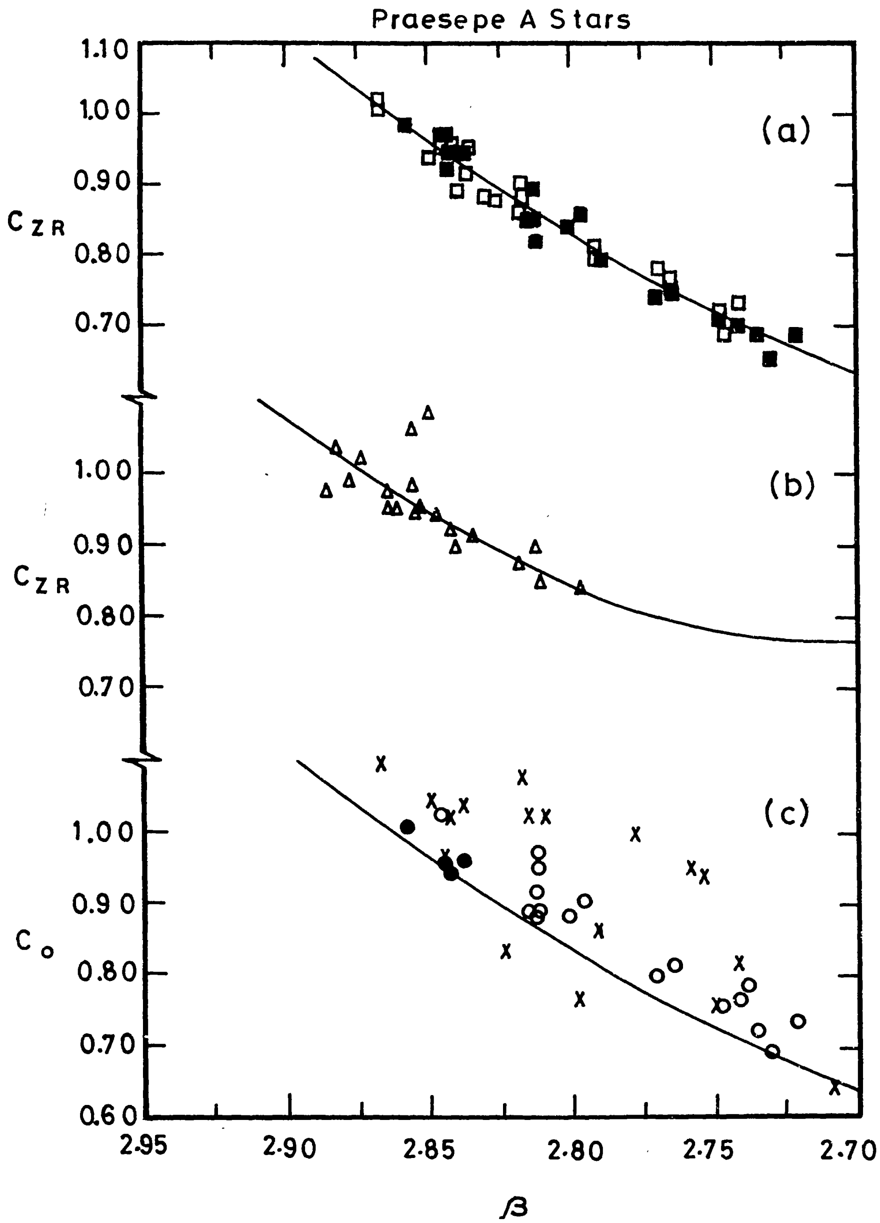

Figure 12. Same as Fig. 10 for the Praesepe cluster. (a) ZRMS values of (β, c_1) of Praesepe stars and the ZRMS curves from observed slopes of rotation effects. (b) ZRMS values of members and ZRMS curve from theoretical slopes of rotation effects. (c) Observed position of stars and the ZRMS curve from observed slopes of rotation effects.

with the m_{1ZR} calculated from the c_{1ZR}, $(b-y)_{ZR}$ and $(u-b)_{ZR}$ derived in earlier sections. We find that for mid-values of β in Table 7 the two agree, while at the two ends of the β range, the differences are of the order of 0.02 magnitudes.

We also calculate m_1 using Method 1b and find that it agrees very well with m_1 calculated from $(b-y)$, $(c_1, u-b)$.

The observed values of β, m_1 and the observed (β_{ZR}, m_{1ZR}) relation for Hyades are shown in Fig. 11(c).

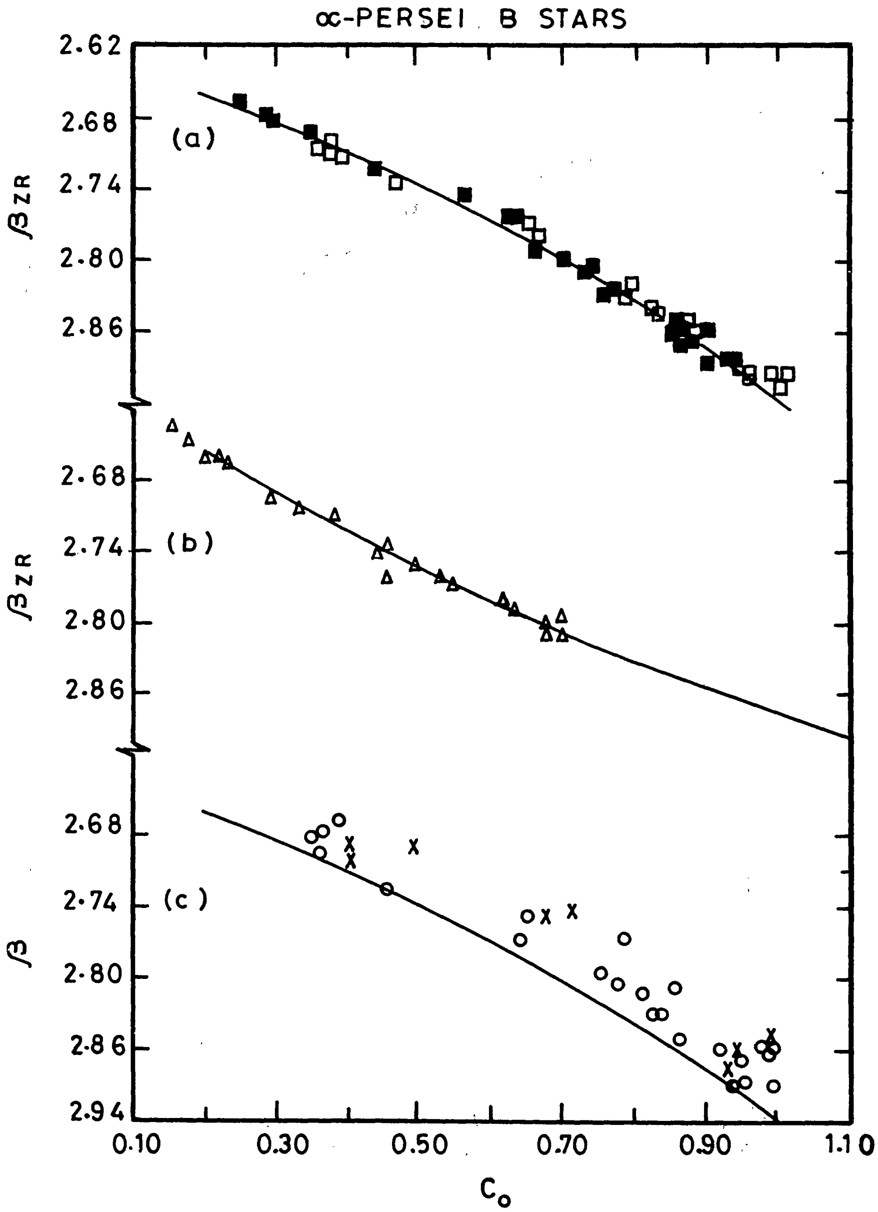

Figure 13. Same as Figs 10 and 12 for α-Persei B stars.

4.4 *ZRMS of Praesepe*

Procedures exactly similar to those followed for Hyades were used to determine the ZRMS of Praesepe. No intersteller extinction corrections are needed for this cluster either. The ZRMS derived from observed rotation effects (Method 1a) is listed in Table 8. The ZRMS values derived from predicted effects from theory (Method 1b) are also listed in Table 8 (Columns 6 to 10). The ZRMS values derived from theory seem to give consistently larger values for all indices (at a given β) for the late A-stars.

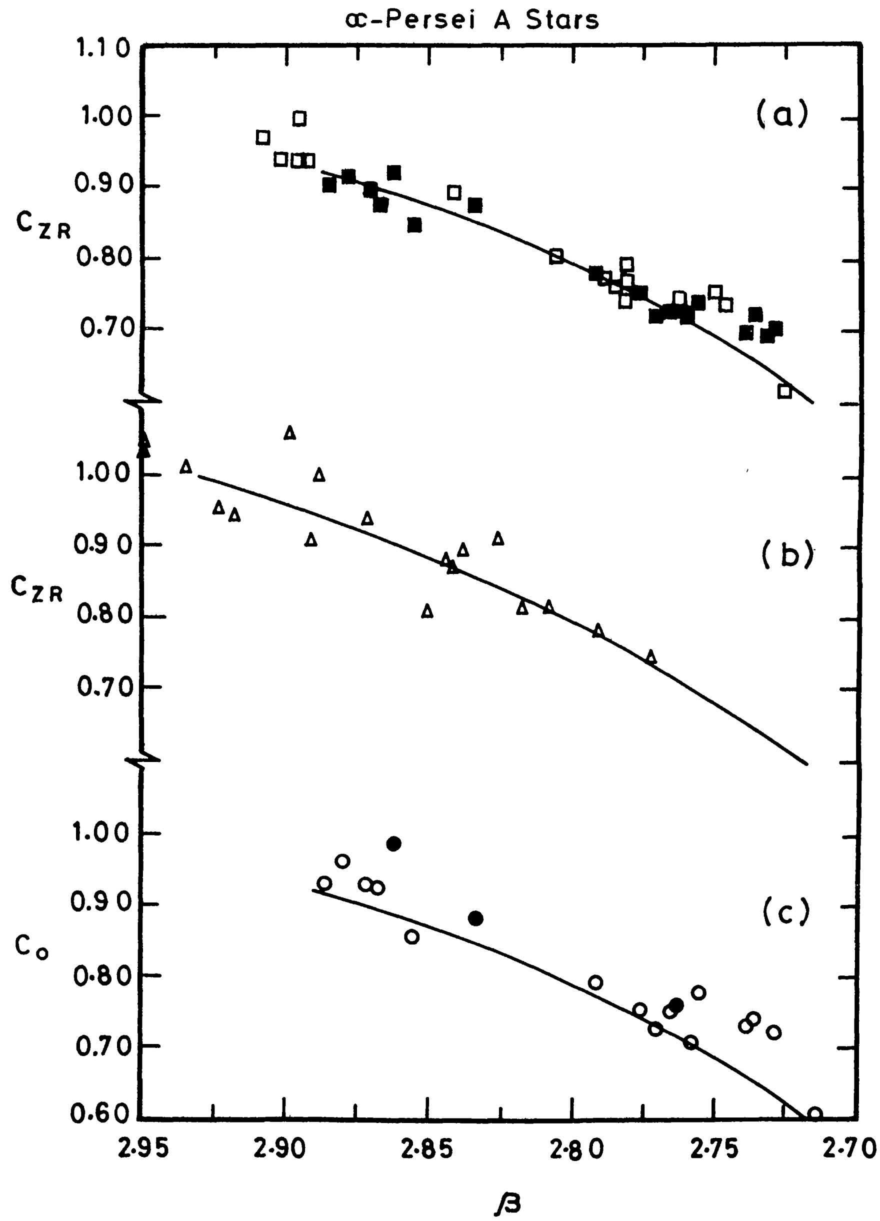

Figure 14. Same as Figs 10 and 12 for α-Persei A stars.

The different diagrams similar to that for Hyades, in the (β, c_1) plane are displayed in Fig. 12.

4.5 *ZRMS Values of α-Persei and Pleiades*

The B stars and A stars were treated separately for determining rotation effects. The methods followed are exactly similar to those for Hyades and Praesepe and we derived the ZRMS value from observed effects (Method 1a) for B stars and A stars independently. The ZRMS values for the B stars in α-Persei are listed in Table 9 and for the A stars in Table 10. We have taken care always to check for the self-consistency of the m_1 values derived.

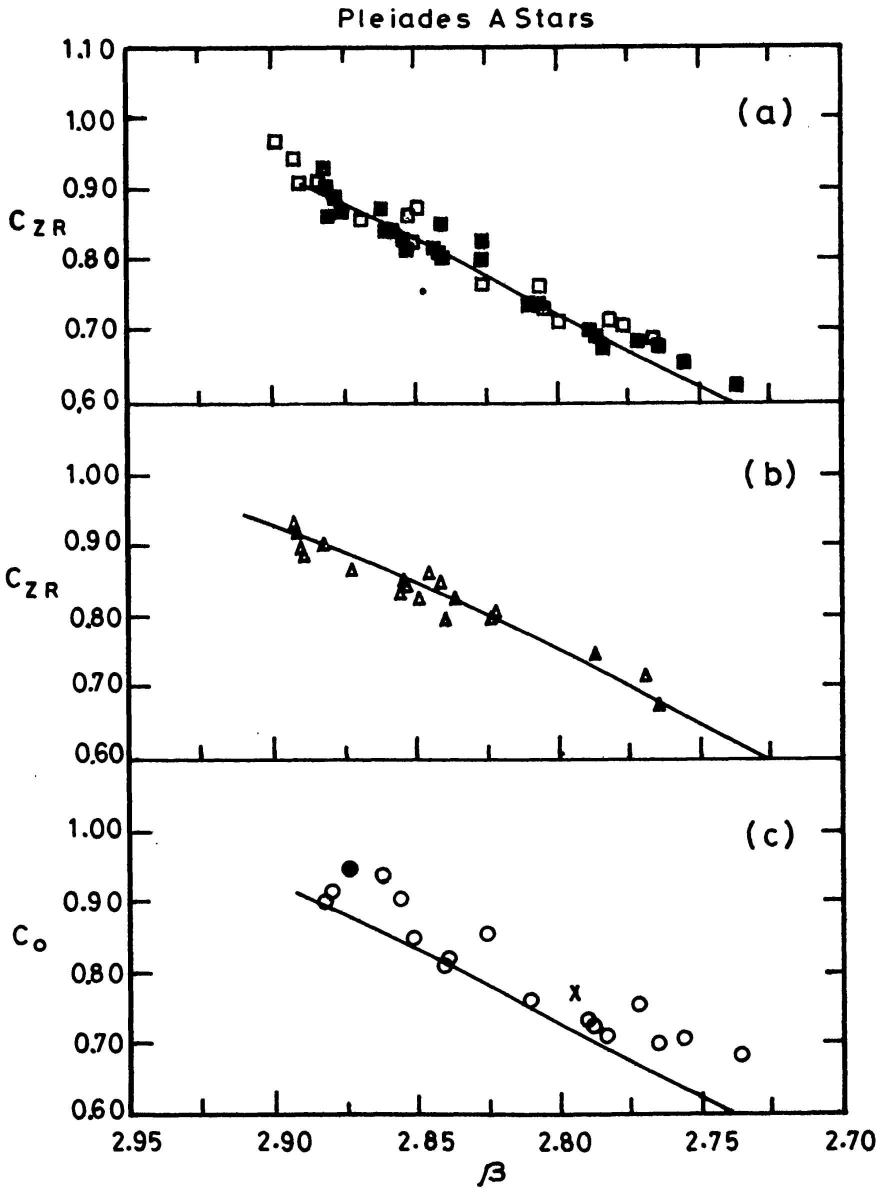

Figure 15. Same as Figs 10 and 12 for Pleiades A stars.

The ZRMS values derived from predicted effects (Method 1b) are listed in Table 9 for B stars and in Table 10 for A stars. The ZRMS values derived from both the methods are found to agree very well with each other.

The ZRMS values are corrected for the average observed intersteller reddening. Extinction corrections are discussed in Section 5 where we discuss the derivation of the Zero Rotation Zero Age Main Sequence (ZRZAMS). In Figs 13 and 14 the different diagrams similar to those for Hyades in the (β, c_1) plane are shown respectively for the B and A stars in α-Persei.

Procedures similar to those for α-Persei were followed for the A-stars in Pleiades and the dereddened ZRMS values derived from observations (Method 1a) and theory (Method 1b) are listed in Table 11. Diagrams similar to those of α-Persei are displayed in Fig. 15 for Pleiades A-stars. The theoretical ZRMS for the B stars in Pleiades are

Table 6. Average change in indices per 100 km s^{-1} of $V\sin i$ ($\omega = 0$; $i = 60°$).

$M/M_\odot$	$(u-b)$	$(b-y)$	$\delta(b-y)$	δM_v	$\delta(u-b)$	δc	δm_1	$\delta\beta$
14.5	−.200	−.150	.007	0.17	.044	.028	.001	.004
11.0	.030	−.118	.008	−.010	.068	.050	.001	.006
8.3	.210	−.098	.009	−.018	.087	.067	.001	.009
6.3	.390	−.078	.010	−.031	.115	.092	.002	.010
4.9	.620	−.059	.012	−.043	.154	.126	.003	.016
3.9	.810	−.045	.013	−.031	.181	.145	.005	.024
3.3	.959	−.034	.017	.009	.191	.144	.007	.029
2.8	1.228	−.015	.026	.106	.178	.115	.006	.022
2.5	1.358	.005	.045	.270	.145	.024	−.006	−.015
2.3	1.433	.026	.050	.311	.057	−.019	−.012	−.031
2.1	1.445	.082	.056	.332	.019	−.055	−.018	−.044
1.9	1.402	.152	.073	.400	−.030	−.118	−.029	−.070
1.8	1.375	.177	.084	.313	−.093	−.181	−.040	−.090
1.7	1.345	.208	.086	.227	−.114	−.203	−.042	−.088
1.5	1.308	.259	.076	.242	−.121	−.206	−.033	−.082

Table 7. Hyades.

β	$(b-y)_0$	m_0	c_0	$(u-b)_0$	M_v	$(b-y)_0$	m_0	c_0	$(u-b)_0$
	Observational ZRMS					Theoretical ZRMS			
2.680	.236	.154	.552	1.332	5.518	.235	.099	.619	1.287
2.690	.231	.160	.569	1.351	5.595	.230	.111	.629	1.311
2.700	.226	.166	.586	1.370	5.659	.224	.123	.640	1.334
2.710	.221	.171	.603	1.387	5.710	.218	.134	.652	1.356
2.720	.215	.177	.622	1.406	5.748	.212	.144	.665	1.377
2.730	.208	.181	.641	1.419	5.773	.205	.154	.678	1.396
2.740	.201	.186	.661	1.435	5.785	.197	.164	.692	1.414
2.750	.194	.190	.682	1.450	5.784	.189	.172	.708	1.430
2.760	.186	.194	.703	1.463	5.770	.181	.180	.724	1.445
2.770	.177	.198	.726	1.476	5.744	.172	.187	.741	1.459
2.780	.168	.201	.749	1.487	5.704	.163	.193	.759	1.472
2.790	.159	.204	.772	1.498	5.651	.153	.200	.777	1.483
2.800	.149	.207	.797	1.509	5.586	.143	.204	.797	1.492
2.810	.138	.209	.822	1.516	5.508	.132	.210	.817	1.501
2.820	.127	.211	.848	1.524	5.416	.121	.214	.839	1.508
2.830	.115	.212	.875	1.529	5.312	.109	.217	.861	1.513
2.840	.103	.214	.902	1.536	5.195	.097	.220	.884	1.518
2.850	.090	.215	.930	1.540	5.065	.084	.222	.908	1.521
2.860	.077	.210	.959	1.533	4.922	.071	.223	.933	1.522
2.870	.062	.215	.989	1.543	4.766	.057	.225	.959	1.523
2.880	.048	.214	1.019	1.543	4.597	.043	.226	.985	1.522
2.890	.033	.213	1.050	1.542	4.415	.029	.224	1.013	1.519
2.900	.016	.212	1.082	1.538	4.221	.014	.223	1.041	1.515

Table 8. Praesepe.

β	$(b-y)_0$	m_0	c_0	$(u-b)_0$	M_v	$(b-y)_0$	m_0	c_0	$(u-b)_0$
	Observational ZRMS					Theoretical ZRMS			
2.680	.253	.148	.605	1.408	2.156	.261	−.018	.752	1.238
2.690	.245	.154	.619	1.418	2.287	.250	.013	.751	1.277
2.700	.236	.161	.633	1.428	2.400	.240	.041	.751	1.313
2.710	.227	.167	.649	1.438	2.494	.230	.067	.753	1.346
2.720	.218	.173	.665	1.448	2.570	.219	.091	.756	1.376
2.730	.208	.179	.683	1.457	2.628	.208	.113	.761	1.404
2.740	.199	.183	.701	1.466	2.667	.198	.133	.767	1.429
2.750	.189	.189	.720	1.475	2.688	.186	.152	.775	1.451
2.760	.179	.193	.740	1.484	2.690	.175	.167	.785	1.470
2.770	.170	.196	.761	1.493	2.674	.164	.182	.795	1.487
2.780	.161	.198	.782	1.501	2.639	.152	.194	.808	1.501
2.790	.151	.201	.805	1.509	2.587	.141	.204	.820	1.512
2.800	.141	.203	.828	1.517	2.515	.129	.212	.837	1.520
2.810	.131	.204	.853	1.524	2.425	.117	.218	.854	1.525
2.820	.122	.205	.878	1.532	2.317	.105	.223	.873	1.528
2.830	.113	.204	.904	1.539	2.191	.093	.225	.893	1.528
2.840	.103	.204	.931	1.546	2.046	.080	.225	.914	1.525
2.850	.095	.202	.959	1.553	1.882	.068	.223	.937	1.519
2.860	·086	.199	.988	1.559	1.701	.055	.219	.962	1.510
2.870	.077	.196	1.018	1.565	1.500	.042	.214	.988	1.499
2.880	.069	.192	1.048	1.571	1.282	.029	.206	1.016	1.485
2.890	.061	.187	1.080	1.577	1.045	.016	.195	1.045	1.468
2.900	.054	.181	1.112	1.583	0.789	.003	.184	1.075	1.449

listed in Table 12. The ZRMS from observations (Method 1a) was not calculated as Pleiades contains only a few single main sequence B-type stars.

4.6 *ZRMS of the Scorpio-Centaurus Association and IC 4665*

As the Upper Scorpius sub-group is known to have highly variable reddening due to interstellar extinction, we decided to consider only the two other subgroups of this association for the derivation of the ZRMS values. The Lower Centaurus and Upper Centaurus subgroups consist mainly of B2 and B3 main sequence stars which gave us the opportunity of deriving accurate rotational effects for this mass range.

The ZRMS values derived from observations and theory (Methods 1a and 1b) for these two subgroups are listed in Table 13. The extinction for this subgroup appears to be extremely small (Glaspey 1971) and therefore needs no correction.

The (dereddened) ZRMS values derived for B-stars of 1C 4665 from observed slopes and theory are given in Table 14.

Table 9. α-Persei B stars.

β	$(b-y)_0$	m_0	c_0	$(u-b)_0$	M_v	$(b-y)_0$	m_0	c_0	$(u-b)_0$
	Observational ZRMS					Theoretical ZRMS			
2.660	−.090	.092	.192	.232	−.919	−.077	.092	.198	.228
2.670	−.089	.092	.233	.277	−.636	−.072	.092	.223	.262
2.680	−.087	.094	.273	.323	−.374	−.069	.093	.250	.297
2.690	−.087	.096	.312	.368	−.134	−.065	.094	.277	.334
2.700	−.085	.097	.350	.414	.086	−.061	.094	.306	.372
2.710	−.081	.099	.388	.459	.284	−.058	.096	.335	.412
2.720	−.079	.101	.424	.505	.460	−.054	.098	.366	.454
2.730	−.076	.103	.461	.550	.616	−.051	.100	.398	.497
2.740	−.071	.105	.496	.596	.750	−.048	.104	.431	.542
2.750	−.068	.107	.530	.641	.863	−.045	.107	.464	.588
2.760	−.064	.110	.564	.687	.954	−.043	.111	.499	.636
2.770	−.060	.111	.597	.732	1.024	−.040	.116	.535	.686
2.780	−.056	.114	.629	.777	1.073	−.037	.120	.572	.737
2.790	−.050	.117	.661	.823	1.101	−.035	.125	.610	.789
2.800	−.045	.119	.692	.868	1.107	−.033	.130	.649	.843
2.810	−.040	.122	.722	.914	1.092	−.031	.136	.689	.899
2.820	−.033	.125	.751	.959	1.056	−.029	.142	.730	.956
2.830	−.027	.127	.779	1.004		−.027	.148	.772	1.015
2.840	−.020	.132	.807	1.050		−.026	.156	.815	1.075
2.850	−.015	.134	.834	1.095		−.024	.163	.859	1.137
2.860	−.006	.138	.860	1.140		−.023	.171	.905	1.201
2.870	−.001	.141	.886	1.185		−.022	.180	.951	1.266
2.880	−.009	.145	.911	1.231		−.021	.188	.998	1.333
2.890	−.018	.149	.935	1.276		−.020	.197	1.047	1.401
2.900	−.027	.152	.958	1.321		−.019	.206	1.096	1.471
2.910	−.035	.156	.980	1.366		−.019	.217	1.146	1.542
2.920	−.045	.160	1.002	1.412					

Table 10. α-Persei A stars.

β	$(b-y)_0$	m_0	c_0	$(u-b)_0$	M_v	$(b-y)_0$	m_0	c_0	$(u-b)_0$
	Observational ZRMS					Theoretical ZRMS			
2.650	.298	.151	.387	1.285	3.720	.304	.143	.389	1.283
2.660	.288	.150	.423	1.298	3.627	.291	.149	.421	1.301
2.670	.278	.149	.457	1.311	3.537	.278	.155	.453	1.319
2.680	.268	.149	.490	1.324	3.449	.266	.160	.484	1.336
2.690	.258	.149	.522	1.336	3.363	.254	.165	.514	1.353
2.700	.248	.150	.553	1.348	3.280	.242	.170	.544	1.368
2.710	.239	.150	.583	1.360	3.199	.230	.175	.572	1.383
2.720	.229	.151	.611	1.371	3.120	.219	.180	.600	1.397
2.730	.219	.152	.639	1.381	3.044	.208	.183	.627	1.410
2.740	.210	.153	.665	1.391	2.970	.197	.188	.653	1.423

Table 10. Continued.

β	$(b-y)_0$	m_0	c_0	$(u-b)_0$	M_v	$(b-y)_0$	m_0	c_0	$(u-b)_0$
	Observational ZRMS					Theoretical ZRMS			
2.750	.200	.156	.690	1.401	2.898	.186	.191	.679	1.434
2.760	.191	.157	.714	1.410	2.829	.176	.195	.703	1.445
2.770	.182	.159	.737	1.419	2.762	.166	.198	.727	1.455
2.780	.172	.163	.758	1.427	2.697	.156	.201	.750	1.464
2.790	.163	.165	.779	1.435	2.635	.146	.205	.772	1.473
2.800	.154	.168	.798	1.442	2.575	.137	.207	.793	1.481
2.810	.145	.172	.816	1.449	2.517	.128	.210	.813	1.488
2.820	.136	.175	.833	1.455	2.462	.119	.212	.833	1.494
2.830	.127	.179	.849	1.461	2.407	.111	.213	.852	1.499
2.840	.118	.184	.864	1.467	2.357	.102	.215	.870	1.504
2.850	.110	.188	.877	1.472	2.310	.094	.216	.887	1.507
2.860	.101	.193	.890	1.477	2.265	.086	.217	.904	1.510
2.870	.092	.198	.901	1.481	2.221	.079	.217	.919	1.512
2.880	.084	.203	.911	1.485	2.180	.072	.218	.934	1.514
2.890	.075	.209	.920	1.488	2.141	.065	.218	.948	1.515

Table 11. Pleiades A stars.

β	$(b-y)_0$	m_0	c_0	$(u-b)_0$	M_v	$(b-y)_0$	m_0	c_0	$(u-b)_0$
	Observational ZRMS					Theoretical ZRMS			
2.680	.253	.172	.467	1.318	3.824	.225	.149	.484	1.231
2.690	.244	.175	.490	1.329	3.687	.218	.158	.508	1.261
2.700	.235	.177	.512	1.337	3.555	.211	.167	.532	1.289
2.710	.226	.180	.534	1.347	3.429	.205	.174	.556	1.315
2.720	.217	.183	.556	1.357	3.308	.198	.182	.579	1.339
2.730	.208	.186	.578	1.367	3.192	.191	.189	.601	1.361
2.740	.199	.189	.600	1.377	3.081	.184	.195	.624	1.381
2.750	.190	.191	.621	1.384	2.976	.176	.200	.646	1.399
2.760	.180	.194	.643	1.392	2.876	.169	.204	.667	1.414
2.770	.171	.197	.664	1.401	2.781	.162	.208	.688	1.427
2.780	.162	.200	.685	1.410	2.691	.154	.211	.709	1.439
2.790	.152	.203	.706	1.417	2.607	.147	.212	.730	1.448
2.800	.142	.206	.727	1.424	2.528	.139	.214	.749	1.455
2.810	.133	.209	.748	1.433	2.455	.131	.214	.769	1.459
2.820	.123	.213	.768	1.441	2.386	.123	.214	.788	1.462
2.830	.113	.216	.789	1.448	2.323	.115	.213	.807	1.463
2.840	.103	.219	.809	1.454	2.265	.107	.211	.825	1.461
2.850	.093	.222	.829	1.460	2.213	.099	.208	.843	1.457
2.860	.082	.225	.849	1.464	2.166	.090	.205	.861	1.451
2.870	.072	.229	.869	1.472	2.124	.082	.200	.878	1.443
2.880	.062	.232	.888	1.477	2.087	.073	.196	.894	1.433
2.890	.051	.235	.908	1.481	2.056	.064	.191	.911	1.421

Table 12. Pleiades B stars.

β	M_v	$(b-y)_0$	m_0	c_0	$(u-b)_0$
		Theoretical ZRMS			
2·640	−1.046	−.111	.103	.258	.242
2.650	−.876	−.107	.101	.276	.265
2.660	−.711	−.103	.100	.294	.289
2.670	−.550	−.099	.101	.312	.315
2.680	−.394	−.095	.101	.332	.343
2.690	−.243	−.091	.101	.351	.371
2.700	−.096	−.087	.102	.372	.401
2.710	.046	−.083	.102	.393	.432
2.720	.184	−.079	.105	.414	.465
2.730	.317	−.076	.107	.436	.499
2.740	.445	−.072	.110	.458	.534
2.750	.569	−.068	.113	.481	.571
2.760	.688	−.064	.116	.504	.608
2.770	.803	−.061	.121	.528	.648
2.780	.913	−.057	.125	.552	.688
2.790	1.019	−.053	.129	.577	.730
2.800	1.120	−.050	.135	.603	.773
2.810	1.216	−.046	.140	.629	.818
2.820	1.308	−.043	.147	.655	.864
2.830	1.395	−.039	.153	.682	.911
2.840	1.478	−.036	.160	.710	.959
2.850	1.556	−.032	.167	.738	1.009
2.860	1.629	−.029	.176	.766	1.060
2.870	1.698	−.025	.184	.795	1.113
2.880	1.762	−.022	.193	.825	1.167
2.890	1.822	−.019	.202	.855	1.222
2.900	1.877	−.015	.212	.885	1.278
2.910	1.928	−.012	.222	.916	1.336

Table 13. Lower-Cen + Upper-Cen B2, B3 stars.

β	$(b-y)_0$	m_0	c_0	$(u-b)_0$	M_v	$(b-y)_0$	m_0	c_0	$(u-b)_0$
	Observational ZRMS					Theoretical ZRMS			
2.600	−.118	.065	−.020	−.125	−3.040	−.122	.081	−.029	−.111
2.610	−.114	.069	.014	−.077	−2.882	−.118	.084	.005	−.063
2.620	−.109	.070	.048	−.029	−2.706	−.115	.088	.037	−.017
2.630	−.105	.073	.081	.018	−2.512	−.111	.091	.067	.027
2.640	−.101	.077	.114	.066	−2.301	−.107	.095	.094	.070
2.650	−.097	.080	.147	.113	−2.071	−.103	.099	.120	.112
2.660	−.093	.084	.179	.160	−1.824	−.099	.104	.143	.152
2.670	−.089	.087	.211	.207	−1.560	−.095	.107	.165	.190
2.680	−.085	.091	.242	.253	−1.277	−.092	.113	.184	.227
2.690	−.082	.095	.273	.300	−.977	−.088	.119	.201	.263
2.700	−.078	.099	.304	.346	−.660	−.084	.125	.216	.297
2.710	−.075	.104	.334	.392	−.324	−.080	.131	.228	.329

Table 14. IC 4665 B stars.

β	$(b-y)_0$	m_0	c_0	$(u-b)_0$	M_v	$(b-y)_0$	m_0	c_0	$(u-b)_0$
	Observational ZRMS					Theoretical ZRMS			
2.680	−.050	.075	.251	.302	−.768	−.050	.076	.309	.361
2.690	−.057	.079	.287	.332	−.736	−.057	.080	.341	.387
2.700	−.063	.083	.323	.365	−.697	−.063	.083	.374	.414
2.710	−.069	.089	.358	.399	−.651	−.069	.088	.406	.444
2.720	−.072	.093	.392	.434	−.598	−.072	.091	.439	.477
2.730	−.075	.097	.426	.472	−.538	−.075	.095	.471	.511
2.740	−.077	.102	.460	.511	−.471	−.077	.100	.503	.549
2.750	−.077	.106	.493	.552	−.397	−.077	.104	.535	.588
2.760	−.076	.110	.526	.595	−.315	−.076	.108	.566	.630
2.770	−.074	.114	.558	.639	−.227	−.074	.112	.598	.674
2.780	−.070	.118	.590	.686	−.132	−.070	.116	.630	.721
2.790	−.065	.120	.622	.733	−.029	−.065	.120	.661	.770
2.800	−.060	.124	.653	.783	.080	−.060	.125	.692	.822
2.810	−.052	.128	.683	.835	.196	−.052	.128	.723	.875
2.820	−.044	.130	.714	.888	.320	−.044	.133	.754	.932
2.830	−.035	.134	.744	.943	.450	−.035	.138	.785	.990
2.840	−.024	.136	.773	.999	.588	−.024	.142	.816	1.051
2.850	−.012	.139	.802	1.058	.732	−.012	.147	.846	1.115
2.860	.001	.142	.830	1.118	.884	−.001	.152	.876	1.181
2.870	.016	.144	.858	1.179	1.042	.016	.155	.907	1.249
2.880	.032	.146	.886	1.243	1.208	.032	.159	.937	1.319
2.890	.049	.148	.913	1.308	1.381	.049	.164	.967	1.392
2.900	.067	.150	.940	1.375	1.560	.067	.178	.997	1.486

5. ZRZAMS

5.1 *Interstellar Reddening*

As both rotation and interstellar extinction redden the stars, we decided to check the $E(b-y)$ values given in the literature for various clusters.

For the A-stars, β and $(b-y)$ are linearly related as both are functions of the effective temperature. Crawford (1977) finds a slight dependence of this relationship on δc_1 and δm_1 terms. The δc_1 term refers to reddening due to evolution and δm_1 the difference in line-blanketing with respect to Hyades values. The largest correction involved due to blanketing differences is of the order of 0.02 magnitudes only. The δc_1 term would be zero for unevolved members.

Rotation does not produce a shift away from the (β, $b-y$) relation whereas extinction would shift the entire sequence along the $(b-y)$ axis only. Hence mean extinction values derived from A-stars in the (β, $b-y$) plane should be independent of rotation effects.

We plotted the ZRMS values of β and $(b-y)$ for various clusters and estimated their relative shift along the $(b-y)$-axis with respect to the Hyades relation. The $E(b-y)$ values derived by us for a few selected clusters were compared with the values quoted in the original papers. The agreement between the two estimates was found to be good excepting for α-Persei where we find our estimate to be smaller by about 0.03 magnitudes. For all the clusters the $E(b-y)$ taken from literature was used for extinction corrections excepting for α-Persei for which we use a value of 0.045 instead of the value 0.07 given by Crawford and Barnes (1974). In Table 15, we list the $E(b-y)$ values and the distance moduli to various clusters taken from the original literature that is listed in Table 1.

5.2 *Absolute Magnitudes*

The distance moduli of the clusters used for deriving the ZRZAMS are also listed in Table 15. These have been taken from the references listed in Table 1. The absolute magnitudes and dereddened colours for all stars were derived using the following relationship (Strömgren 1966).

$$E(b-y) = 0.70\,E(B-V)$$

$$E(m_1) = -0.18\,E(b-y)$$

$$E(c_1) = 0.20\,E(b-y)$$

$$E(u-b) = 1.84\,E(b-y)$$

$$A_v = 4.57\,E(b-y).$$

The ZRMS values listed in Section 4 have all been corrected for average extinction using the above relationship.

5.3 *ZRZAMS: From Observed Slopes of Rotation Effects*

The ZRMS values of various indices as a function of β derived for different clusters were all superposed to derive the mean ZRZAMS for B and A stars separately. In Fig. 16 we show in the (β, c) plane the ZRMS curves for B stars of α-Persei, Upper Centaurus and IC 4665. A similar diagram for the A stars is shown in Fig. 17 where the values for stars in α-Persei, Pleiades, Hyades and Praesepe are plotted. ZRMS

Table 15. $E(b-y)$ & distance modulus for clusters.

Cluster	$E(b-y)$ literature	$m-M$	Cluster	$E(b-y)$ literature	$m-M$
Hyades		3.2	NGC 2422	0.06	8.01
Praesepe	< 0.01	6.1	Coma	—	4.5
α-Persei	0.07	6.1	IC 2602	0.021	5.94
Pleiades	0.04	5.54	Cep OB3	0.6	9.3
Upper-Cen		6.0	NGC 2287	0.018	9.10
IC 4665	0.14	7.5	NGC 6475	0.067	7.02
NGC 2516	0.088	8.01	NGC 2244	0.34	10.96
IC 4756	0.161	8.05	h & χ-Persei	0.41	11.8
NGC 2264	0.057	9.5	NGC 4755	0.28	11.4
IC 2391	0.000	5.90			

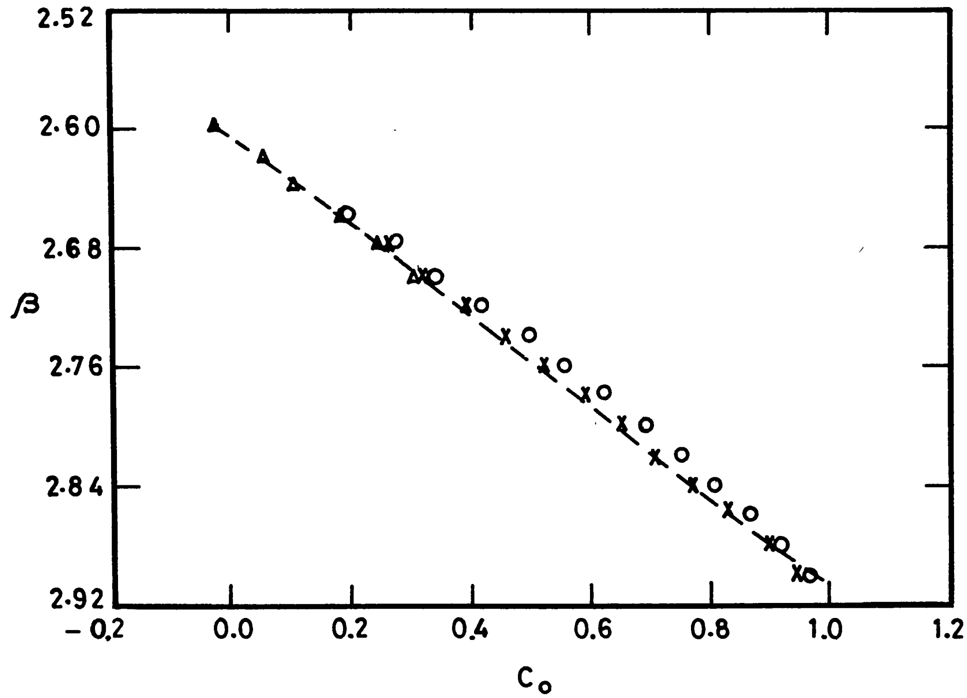

Figure 16. The ZRMS curves in the (β, c_0) plane determined from observed rotational effects for α-Persei B stars, Lower and Upper Centaurus B2, B3 stars and IC 4665 B-stars are shown. The adopted ZRZAMS values of c_0 as a function of β are shown by a dotted line.

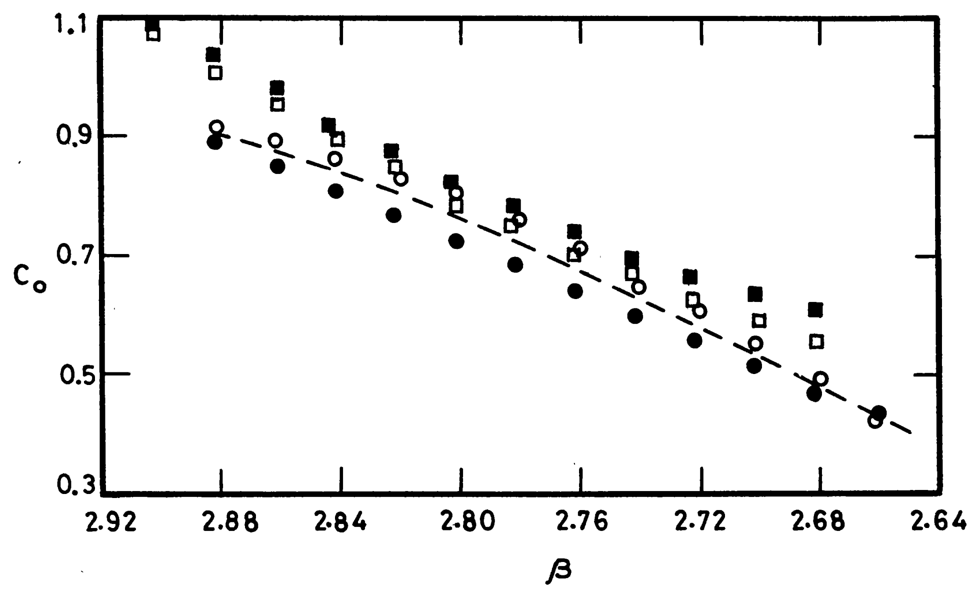

Figure 17. Same as Fig. 16 for A-stars. The ZRMS from observed slopes of rotation effects of α-Persei, Pleiades, Hyades and Praesepe are plotted. The adopted ZRZAMS curve is shown by a dotted line.

values for the B and A stars are plotted in the $(\beta,\ b-y)$, and $(\beta,\ u-b)$ planes respectively in Figs 18 and 19. Preliminary ZRZAMS values derived from this set of clusters are listed in Tables 16 and 17 for B and A stars respectively. We expect

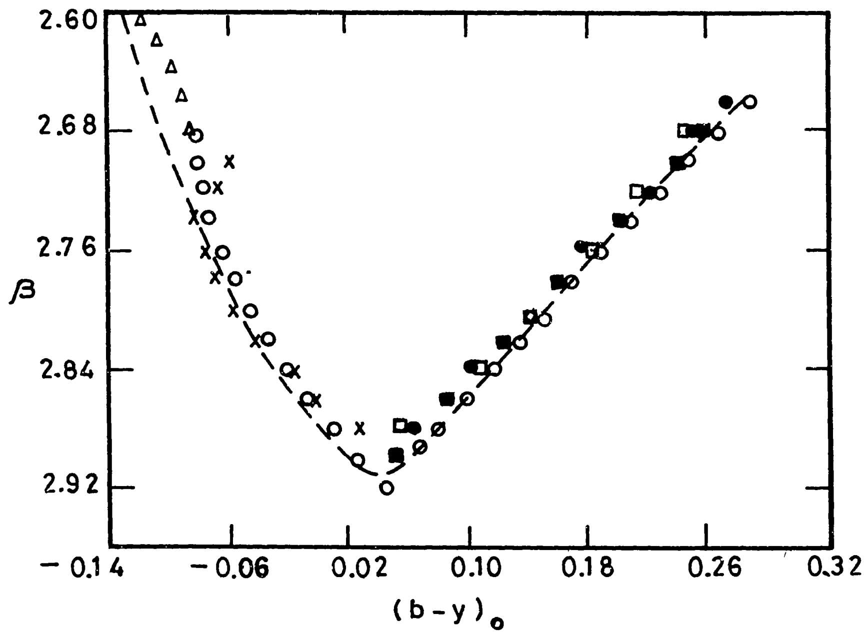

Figure 18. The ZRMS (observational) in the (β, $b-y$) plane for A and B-type stars of all clusters plotted in Figs 16 and 17 is shown. The adopted ZRZAMS values of ($b-y$) as a function of β are shown by the dotted line.

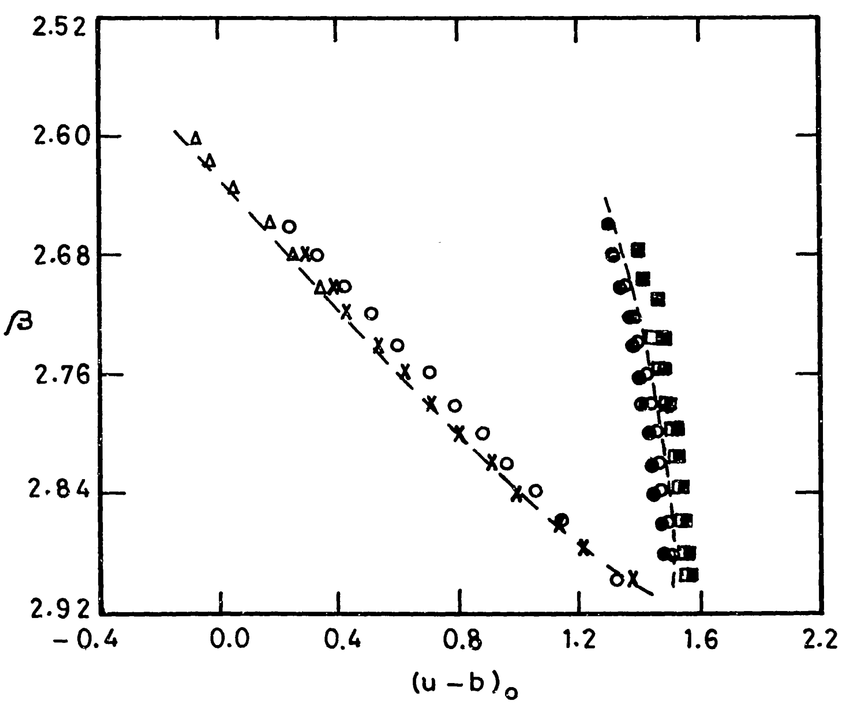

Figure 19. Same as Fig. 18 in the ($\beta, u-b$) plane.

that this would be highly representative of the true values from mid-B to late A and early F star ranges. The B2, B3 type stars are represented only by the Lower Centaurus and Upper Centaurus group.

5.4 *ZRZAMS: From Theoretical Corrections*

ZRZAMS from theoretical corrections also was derived by superposing the theoretical ZRMS curves for various clusters. In addition to α-Persei, Pleiades, Hyades, Praesepe, Upper Centaurus and IC 4665, we have used Cep OB3, Coma, IC 2602, IC 2391, IC 4756, NGC 2264, NGC 2516 and NGC 4755 to check the derived ZRZAMS by

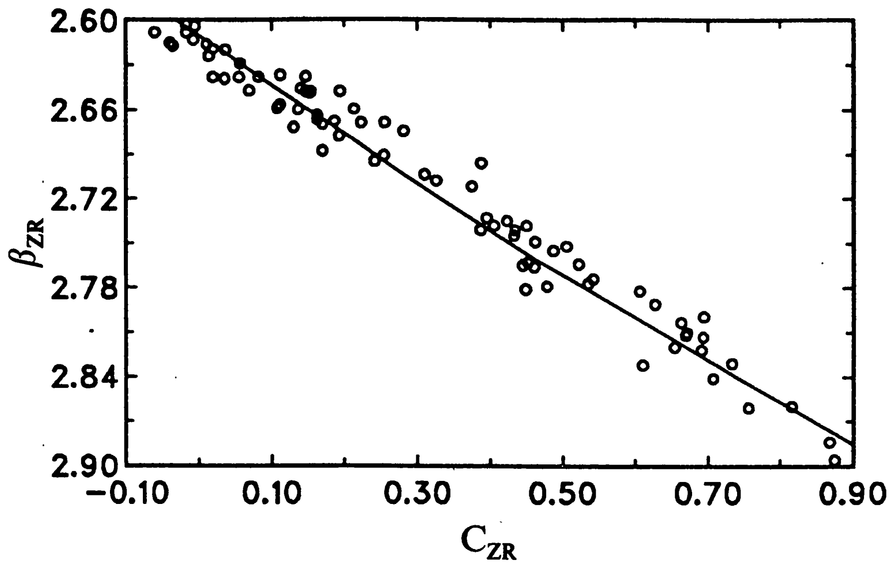

Figure 20. The theoretically corrected values of β and c_0 for B-stars in various cluster stars with $V \sin i \geqslant 100\,\mathrm{km\,s^{-1}}$ have been plotted. The adopted ZRZAMS theoretical curve is shown as a line.

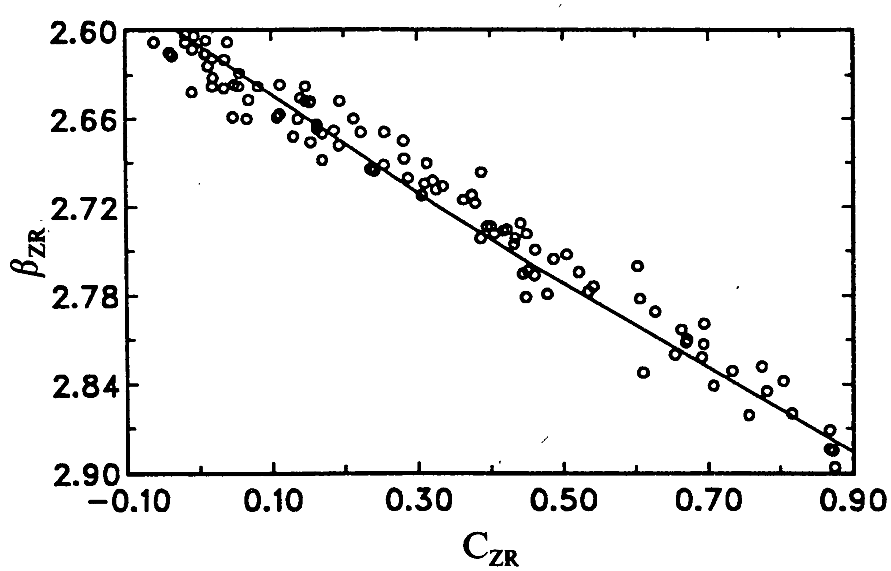

Figure 21. Same as Fig. 20. Stars with all $V \sin i$ values have been plotted.

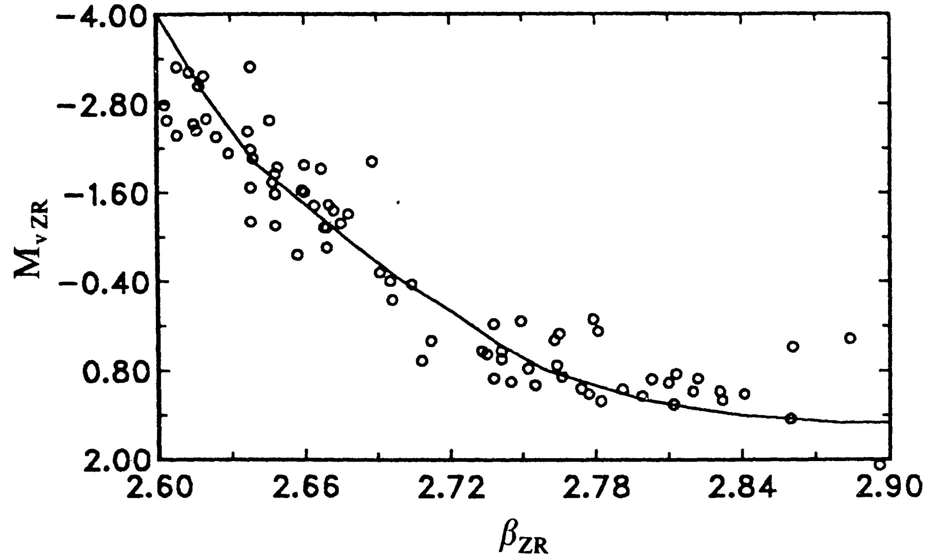

Figure 22. The theoretically corrected values of M_v and β for B stars, with $V\sin i \geqslant 100\,\mathrm{km\,s^{-1}}$, in various clusters have been plotted. The adopted ZRZAMS curve (theoretical) is shown as a line.

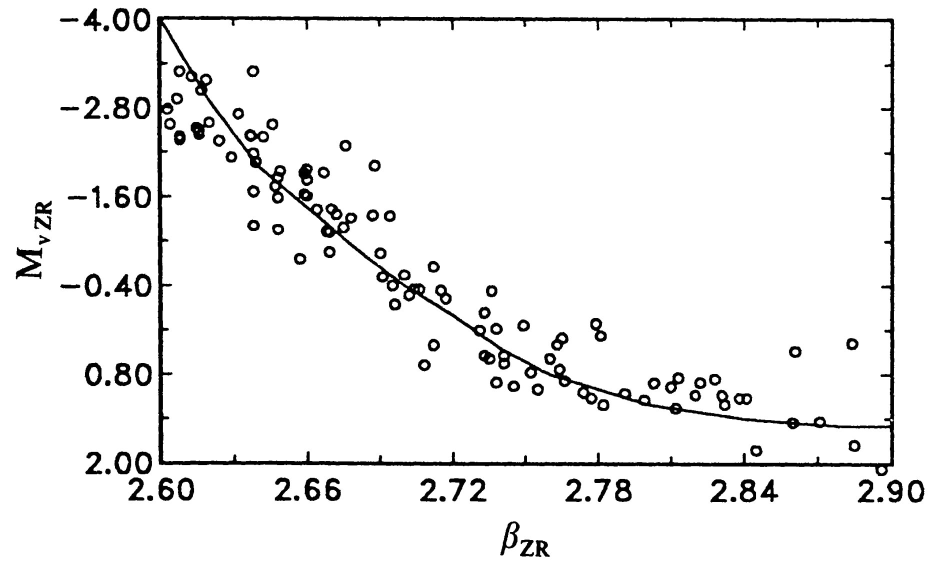

Figure 23. Same as Fig. 22. Stars with all $V\sin i$ values have been plotted.

correcting the indices using the theoretical predictions of Collins & Sonneborn for $i = 60°$.

Because we are assuming a value of $i = 60°$ for all stars, we are likely to leave uncorrected, all such stars which are rotating fast but seen pole-on. For example, in an M_v versus c_0 plane for B-stars, these will be more than half a magnitude above the non-rotators at a given c_0. These objects would add to the scatter that would be introduced by the inclusion of visual and double-lined spectroscopic binaries.

We checked the derived ZRZAMS values using stars that have V sin i values greater than or equal to $100\,\mathrm{km\,s^{-1}}$. We compared these determinations with those derived by using all stars without any discrimination. Fig. 20 shows, for fast rotating

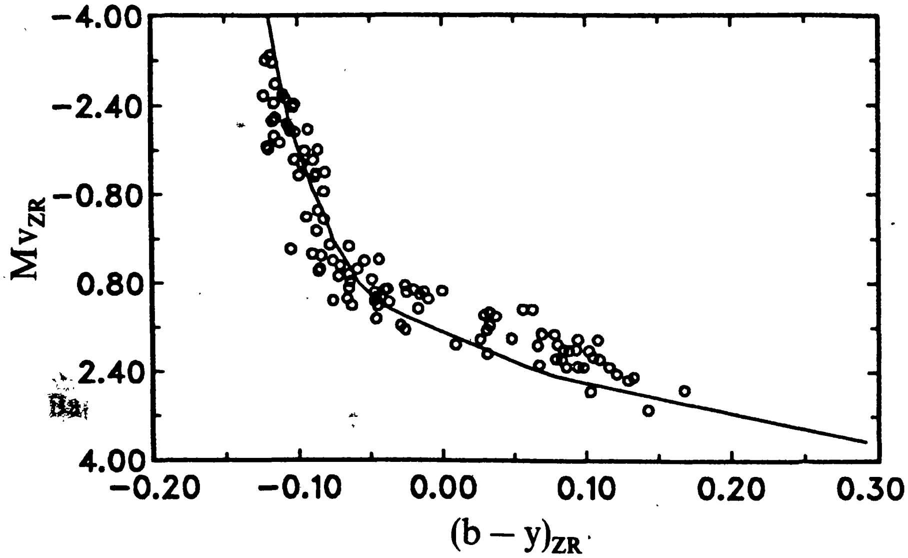

Figure 24. The theoretically corrected values of M_v and $(b-y)$ for B and A stars, with $V\sin i \geqslant 100\,\mathrm{km\,s^{-1}}$, in various clusters have been plotted. The adopted ZRZAMS (theoretical) curve is also shown.

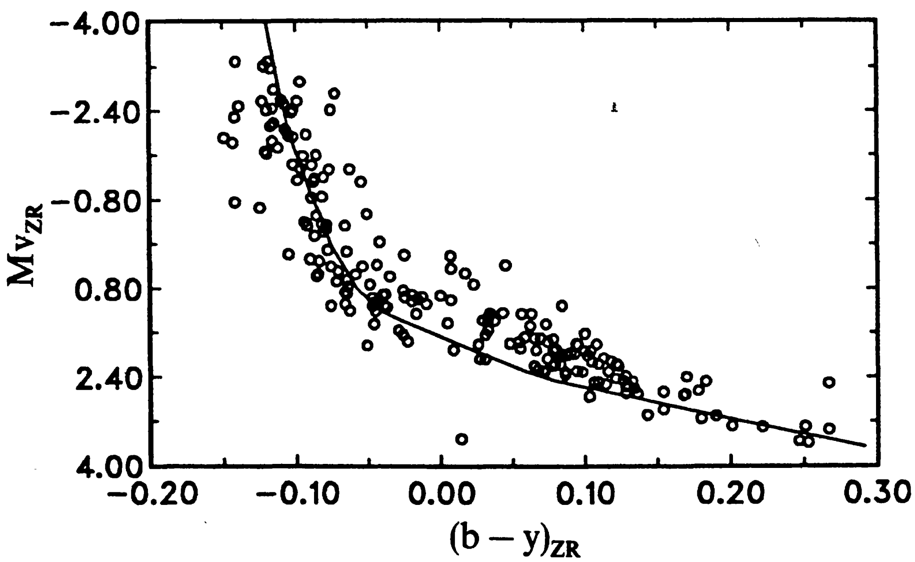

Figure 25. Same as Fig. 24. Stars with all $V\sin i$ values have been plotted.

($V \sin i \geqslant 100\,\mathrm{km\,s^{-1}}$) B stars, the plot of β_{ZR} and c_{ZR} values corrected for rotation. The theoretical ZRZAMS curve is also shown. The relationship appears extremely smooth as expected. In Fig. 21 stars of all $V \sin i$ values are plotted. α-Persei, Pleiades, Upper and lower Centaurus, Cep OB 3, IC 4665, IC 2602, IC 2391, NGC 2264 and NGC 4755 have been included. Similar diagrams in the (M_v, β) and (M_v, $b-y$) planes are shown in Figs 22–27. Fig. 26 is a plot of β_{ZR}, $(b-y)_{ZR}$ for stars of all $V \sin i$ values and $(c_{ZR}, u-b)_{ZR}$, for fast rotators is plotted in Fig. 27.

Similarly from a superposition of various clusters containing A-stars the ZRZAMS values were determined. The following clusters were used; α-Persei, Pleiades, Hyades, Praesepe, IC 4665 and Coma. The theoretical ZRZAMS values are also listed in

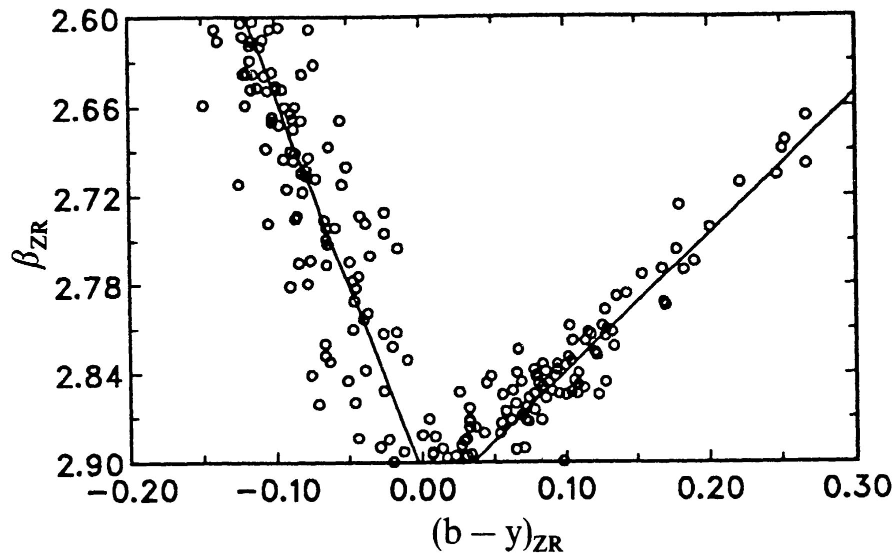

Figure 26. The theoretically corrected values of β and $(b-y)$ for B and A stars in various clusters have been plotted. The adopted ZRZAMS (theoretical) values are shown by lines.

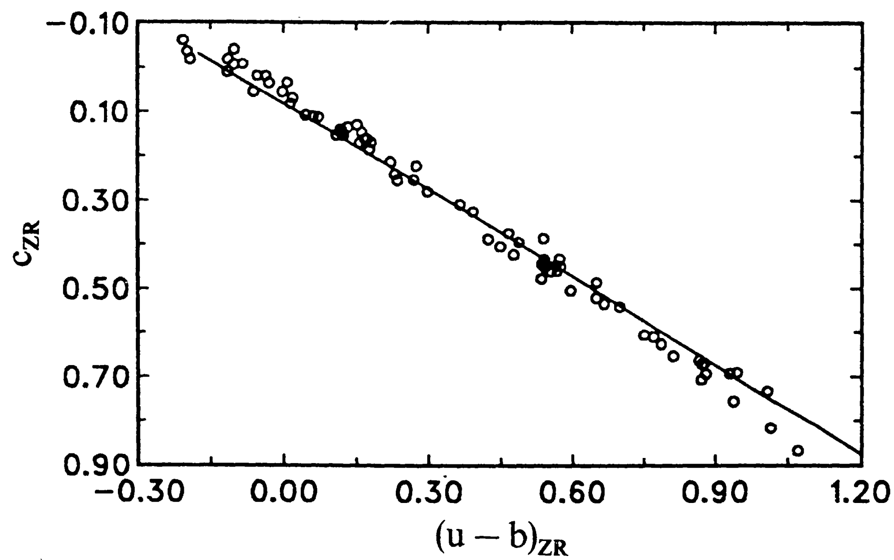

Figure 27. The theoretically corrected c_0 and $(u-b)_0$ values for cluster B-stars with $V\sin i \geqslant 100\,\mathrm{km\,s^{-}}$ have been plotted. The adopted ZRZAMS values (theoretical) are shown by a line.

Tables 16 and 17 for B and A stars respectively. Adopted ZRZAMS values are the averages of the observational and theoretical ZRZAMS values and are listed in Tables 18 and 19 for B and A-type stars respectively.

A comparison of our adopted ZRZAMS values is made with the zero age main sequence values derived by Crawford (1975, 1978, 1979). Crawford has listed the ZAMS values derived from the locus of the blue envelope of B and A stars. We can easily anticipate that such a blue envelope should also represent the zero rotation zero age main sequence and hence must agree with our values derived by correcting for rotation effects. In Figs 28–30 we have compared these two independent determin-

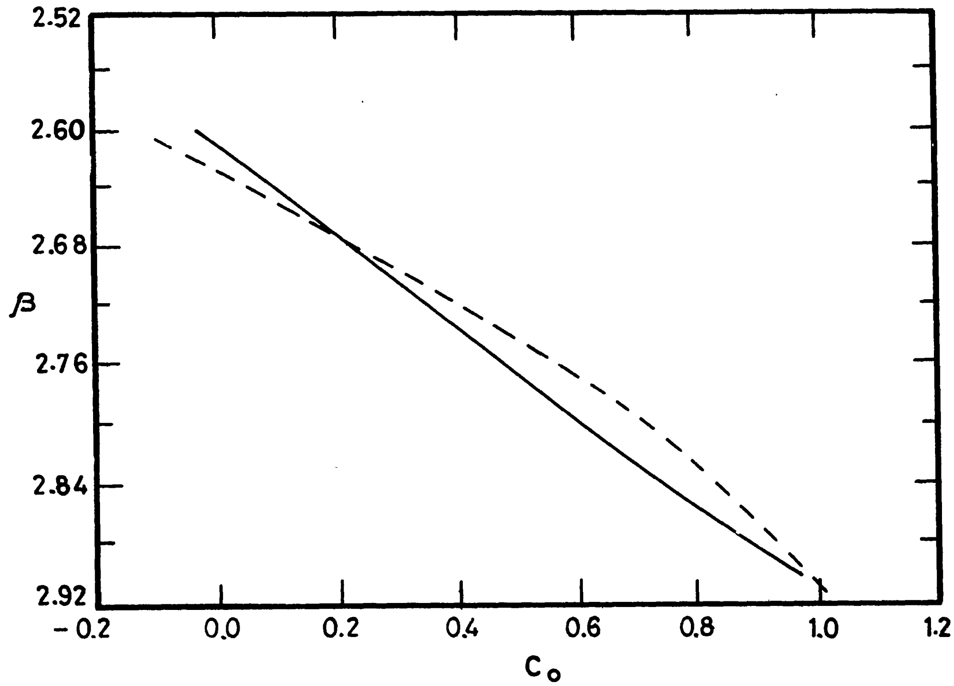

Figure 28. The ZRZAMS values for B stars derived in this study are compared with the values derived by Crawford (1978, 1979) from the lower envelope of field and cluster stars (dotted line), in the β, c_0 plane.

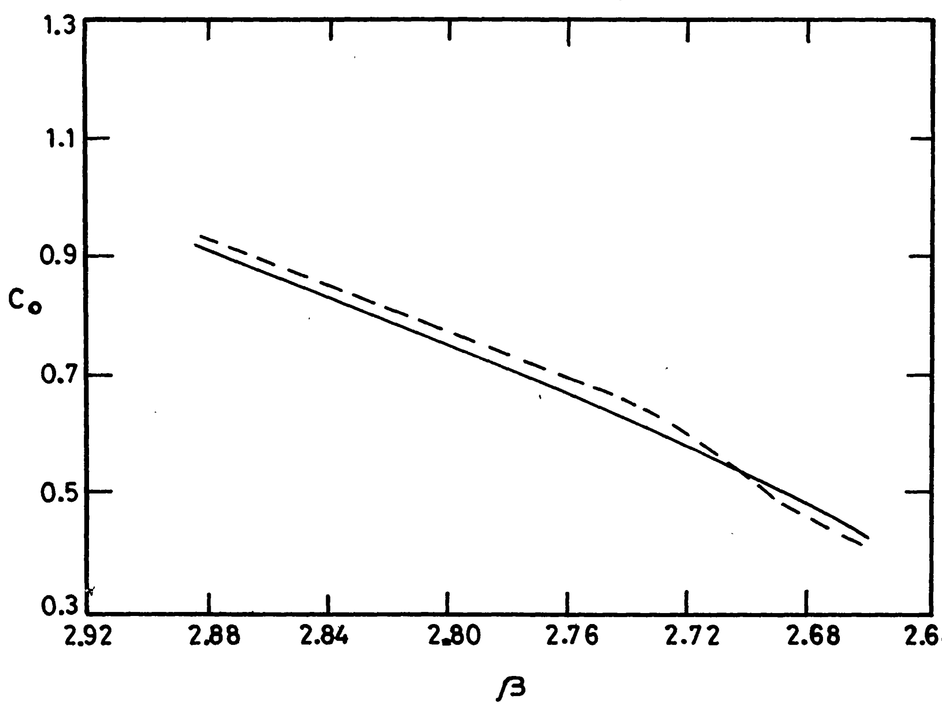

Figure 29. Same as Fig. 28 for A-type stars.

ations. The agreement is excellent and supports the fact that rotation affects all the observed parameters and our procedures in determining the ZRZAMS values should be valid.

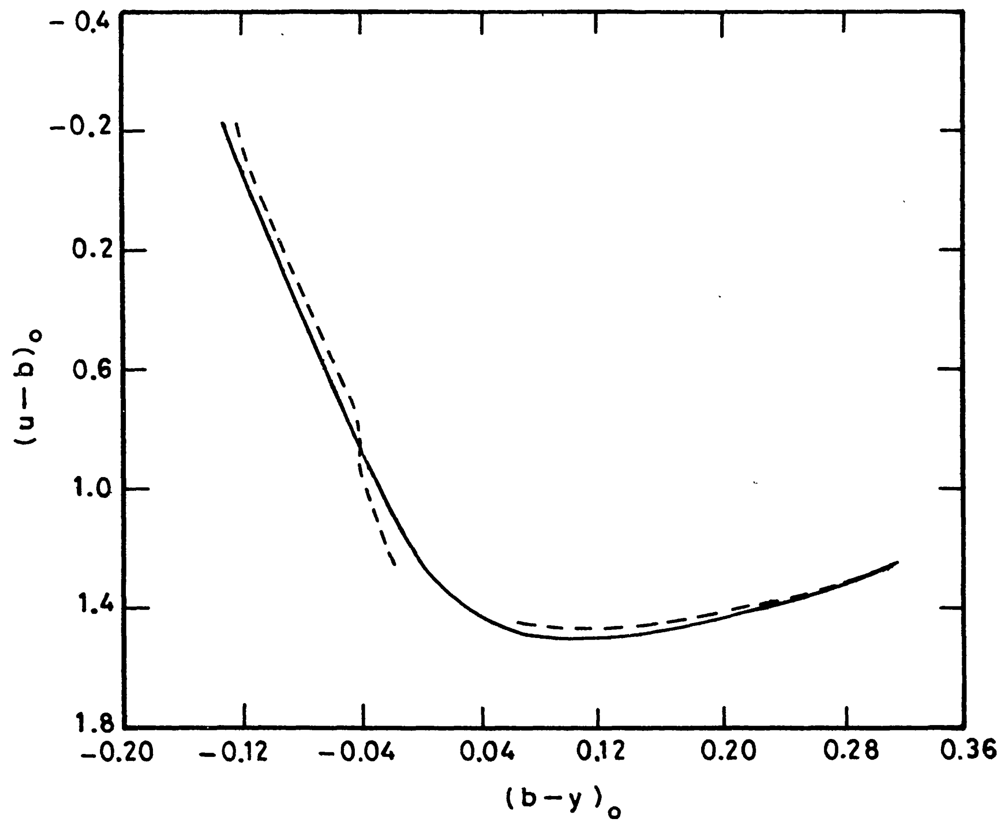

Figure 30. Same as Figs 28 and 29 in the $(u-b, b-y)$ plane for B and A-type stars.

Table 16. B-type stars.

β	$(b-y)_0$	m_0	c_0	$(u-b)_0$	M_v	$(b-y)_0$	m_0	c_0	$(u-b)_0$
	Observational ZRMS					Theoretical ZRMS			
2.60	−.130	0.067	−0.020	−0.146	−4.00	−0.120	0.047	−0.030	−0.175
2.62	−.125	0.073	0.046	−0.058	−2.90	−0.112	0.056	0.030	−0.082
2.64	−.118	0.079	0.111	−0.033	−2.00	−0.104	0.065	0.090	0.012
2.66	−.110	0.084	0.177	0.125	−1.45	−0.097	0.074	0.150	0.104
2.68	−.102	0.090	0.243	0.219	−0.90	−0.090	0.083	0.210	0.196
2.70	−.094	0.096	0.308	0.312	−0.40	−0.081	0.092	0.270	0.292
2.72	−.087	0.102	0.374	0.404	0.00	−0.073	0.101	0.330	0.386
2.74	−.080	0.108	0.440	0.496	0.45	−0.066	0.110	0.395	0.483
2.76	−.071	0.114	0.506	0.592	0.80	−0.058	0.119	0.460	0.582
2.78	−.062	0.120	0.571	0.687	1.00	−0.050	0.128	0.530	0.686
2.80	−.057	0.128	0.637	0.791	1.20	−0.042	0.136	0.600	0.788
2.82	−.040	0.137	0.702	0.896	1.30	−0.034	0.145	0.670	0.892
2.84	−.028	0.146	0.768	1.004	1.40	−0.026	0.154	0.740	0.996
2.86	−.014	0.155	0.834	1.116	1.50	−0.019	0.163	0.810	1.108
2.88	.002	0.166	0.900	1.236	1.75	−0.011	0.172	0.880	1.202
2.90	.020	0.176	0.966	1.358	1.80	−0.003	0.183	0.950	1.310

Table 17. A-type stars.

β	$(b-y)_0$	m_0	c_0	$(u-b)_0$	M_v	$(b-y)_0$	m_0	c_0	$(u-b)_0$
	Observational ZRZAMS					Theoretical ZRZAMS			
2.64						0.312	0.133	0.405	1.295
2.66	0.281	0.157	0.422	1.298	3.66	0.291	0.144	0.448	1.318
2.68	0.262	0.164	0.478	1.330	3.54	0.270	0.155	0.491	1.341
2.70	0.242	0.172	0.532	1.360	3.42	0.249	0.166	0.533	1.363
2.72	0.223	0.179	0.583	1.387	3.30	0.228	0.176	0.577	1.385
2.74	0.205	0.186	0.632	1.414	3.18	0.206	0.186	0.620	1.404
2.76	0.186	0.194	0.678	1.438	3.06	0.185	0.196	0.662	1.424
2.78	0.168	0.199	0.721	1.455	2.94	0.163	0.203	0.705	1.437
2.80	0.151	0.205	0.762	1.474	2.82	0.142	0.209	0.748	1.450
2.82	0.133	0.211	0.800	1.488	2.70	0.120	0.214	0.791	1.459
2.84	0.115	0.215	0.836	1.496	2.58	0.099	0.218	0.834	1.468
2.86	0.096	0.219	0.870	1.500	2.46	0.078	0.221	0.877	1.475
2.88	0.078	0.222	0.900	1.500	2.28	0.057	0.222	0.920	1.478
2.90		0.225				0.036	0.221	0.970	1.484

Table 18. Adopted ZRZAMS for B-type stars.

β	M_v	$(b-y)_0$	m_0	c_0	$(u-b)_0$
2.60	−4.00	−0.125	0.057	−0.025	−0.161
2.62	−2.90	−0.119	0.065	0.038	−0.070
2.64	−2.00	−0.111	0.072	0.100	0.023
2.66	−1.45	−0.104	0.079	0.164	0.115
2.68	−0.90	−0.096	0.087	0.226	0.208
2.70	−0.40	−0.088	0.094	0.289	0.302
2.72	0.00	−0.082	0.102	0.352	0.392
2.74	0.45	−0.073	0.109	0.417	0.490
2.76	0.80	−0.065	0.117	0.483	0.587
2.78	1.00	−0.056	0.124	0.550	0.687
2.80	1.20	−0.050	0.132	0.618	0.790
2.82	1.30	−0.037	0.141	0.686	0.894
2.84	1.40	−0.027	0.150	0.754	1.000
2.86	1.50	−0.017	0.159	0.822	1.112
2.88	1.75	−0.005	0.169	0.890	1.219
2.90	1.80	0.009	0.180	0.958	1.334

Table 19. Adopted ZRZAMS for A-type stars.

β	M_v	$(b-y)_0$	m_0	c_0	$(u-b)_0$
2.66	3.66	0.286	0.150	0.435	1.308
2.68	3.54	0.266	0.160	0.484	1.336
2.70	3.42	0.246	0.169	0.532	1.362
2.72	3.30	0.226	0.178	0.580	1.386
2.74	3.18	0.206	0.186	0.626	1.409
2.76	3.06	0.186	0.195	0.670	1.431
2.78	2.94	0.166	0.201	0.713	1.446
2.80	2.82	0.148	0.207	0.755	1.462
2.82	2.70	0.127	0·212	0.795	1.469
2.84	2.58	0.107	0.216	0.835	1.482
2.86	2.46	0.087	0.220	0.874	1.488
2.88	2.28	0.068	0.222	0.910	1.489

6. Discussion

We have established firmly the rotation effects in the intermediate band photometric indices for various mass ranges by analysing a large number of clusters for which sufficient data are available. This was possible because the method we followed took care of most of the complications that would have otherwise been introduced by causes other than rotation. In principle, this method is similar to the one followed by Strittmatter (1966) in his analysis of the Praesepe cluster. Stritttmatter measured ΔV at a given $(B-V)$ value, where ΔV was defined as the difference between the observed and assumed zero rotation main sequence value of the V-magnitude. But we did not wish to make any assumption on the ZRMS values, instead we decided to derive it after determining the rotation effects. This is where we departed in the data analysis from the earlier workers in the field. For example, Crawford & Barnes (1974) measured the deviations in c_1 from a preliminary calibration of ZAMS. In the α-Persei cluster, they found the deviation in c_1 for A-stars to show rotation effects while the B-star data appeared to be unaffected by rotation. Instead of assuming a ZRMS or ZAMS values, we derived for each cluster a mean main sequence from which the deviations were measured. Our approach clearly demonstrates the rotation effects for both B and A-stars (Rajamohan & Mathew 1988, Mathew & Rajamohan 1990a, b). Likewise Warren's (1976) analysis of Orion association failed to reveal the rotation effects for $V \sin i$ values less than $250\,\mathrm{km\,s^{-1}}$. Although the analysis of field stars by Hartwick & Hesser (1974) and by Gray & Garrison (1988, 1989, 1990) demonstrates the rotation effects on β and c_1, the spread is large as they have not taken into account the reddening by other causes. The causes for the conflicting results of earlier analysis of observational data can be traced to an assumption of an assumed calibration that does not take rotation into account together with the effects of evolution which causes a large spread when objects of different ages are pooled together. The smallness of the rotation effects for moderate rotational velocities, and the fact that rotation effects are a function of mass m, true rotational velocity V and the inclination i of the rotation axis to the line of sight (whereas only $V \sin i$ is observable) introduces further uncertainties in any analysis of data.

Our analysis has established not only the reality of rotation effects on observable parameters but also that the agreement is near perfect with the theoretical calculations, especially of Collins and his co-workers.

The analysis of B2, B3 stars of Upper and Lower Centaurus, the B5 to B9 stars of α-Persei, and IC 4665, the A3-F2 stars of α-Persei, Pleiades, Hyades and Praesepe clearly demonstrates this agreement with the predicted values by Collins & Sonneborn (1977). The A0-A2 type stars have not been analysed. This is a spectral domain in which almost all indices are a function of both the effective temperature and gravity. Further, the procedures we adopted are not suitable for this spectral type range. At these types both β and c reach a maximum value and the rotation effect on $(u-b)$ starts reducing here after reaching a maximum around B9—while the effect on $(b-y)$ starts becoming more pronounced.

A basic assumption which underlies all our calculations is that the rotation effects are linear. This is not true for values of $\omega > 0.9$. The early B-stars, where the Be phenomenon is known to be pronounced, appear to rotate with $\omega > 0.9$ when they arrive on the main sequence (Rajamohan 1978). The ZRMS and ZRZAMS values in this paper would be slightly uncertain in the B0–B3 range. We have also not determined directly the rotation effects on M_v from observations. As theory and observations agreed for all other indices, we have used the theoretical predictions to derive ZRZAMS values of M_v as a function of β. The agreement with Crawford's (1978) determination of the β, M_v values for the blue envelope of B-stars tends to confirm the theoretical predictions of Collins and Sonneborn. However, having determined ZRZAMS values after first establishing the rotation effects, it should now be possible to use all the unevolved members of the galactic clusters to establish firmly the rotation effects on M_v.

7. Summary and conclusions

Effects of rotation on the intermediate band indices *uvby* and H_β are firmly established empirically from published data for many clusters. The observed positions of single main sequence stars and single-lined spectroscopic binaries in a given plane defined by any two of the indices were used to establish the relative displacements due to rotation.

As interstellar extinction also reddens the stars, the Alpha Persei Cluster was analysed using both observed and dereddened indices. It was found that for Alpha Persei, where non-uniformity of extinction is not large, both reddened and dereddened indices lead to similar results. However, as suggested by Gray and Garrison, we used the observed indices for other clusters as dereddening procedures for A-stars are based on an assumed calibration which may be in error due to rotational reddening.

Evolutionary effects will introduce a scatter if the cluster members are not coeval. This is evident from our results for the Scorpio-Centaurus association. Here the Upper Scorpius members which are younger than the Lower Centaurus and Upper Centaurus subgroups were found to be separated in all diagrams of colour excess due to reddening versus $V \sin i$ diagrams (Mathew & Rajamohan 1990a). Also the scatter for Upper Scorpius was large where the interstellar extinction is highly non-uniform. The Upper Centaurus and Lower Centaurus groups which are unreddened, consisting mostly of B2 and B3 type-stars show the reddening effect due to rotation in perfect agreement with theoretical predictions by Collins & Sonneborn (1977) for stars in the similar mass range.

As the predicted effects are a function of the mass, we analysed all clusters grouping them into three ranges corresponding to the spectral type ranges B0–B3, B5–B9 and A3–F0. The predicted indices for these ranges by Collins and Sonneborn were analysed the same way as was done for our observational data.

In our analysis of the theoretically derived indices we did not assume any distribution in v or i. Instead, for each value of i (30°, 45°, 60° and 90°) we took sixteen values corresponding to $\omega = 0.2$, 0.5, 0.8 and 0.9 for the mass range corresponding to the spectral types from B0–B3, B5–B9 and A3–F0 and derived the rotation effects in different planes (such as β, c_1, β, $(u-b)$ etc.). We found that the rotation effects determined from observed data points for clusters, very closely matched the predictions for the various mass ranges. We have established very firmly that not only rotation effects can be discerned from observations but also that the agreement is excellent with theoretical predictions of Collins & Sonneborn (1977) for rigidly rotating stars.

The observed rotation effects, together with theoretical predictions were used to derive ZRMS for various clusters. The sequences were combined to derive preliminary ZRZAMS values of the various indices.

Acknowledgements

All computations for this work was carried out with the Mighty Frame Computer located at the IIA campus. We are thankful to A. V. Raveendran and B. A. Varghese for the help they have rendered at the computer. One of us (Annamma Mathew) is thankful to the University Grants Commission, New Delhi for their grant under the Faculty Improvement Programme with which this work was carried out.

References

Abney, W. de W. 1877, *Mon Not. R. astr. Soc.*, **37,** 278.
Abt, H. A. 1970, in *IAU Coll. 4:* Steller Rotation, Ed. A. Slettebak, D. Reidel, Dordrecht, p. 193.
Abt, H. A., Chaffee, F. H. 1967, *Astrophys. J.*, **148,** 459.
Abt, H. A., Clements, A. E. Doose, L. R., Harris, D. H. 1969, *Astr. J.*, **74,** 1153.
Abt, H. A., Jewsbury, C. P. 1969, *Astrophys. J.*, **156,** 983.
Abt, H. A., Levato,. H. 1977, *Publ. astr. Soc. Pacific*, **89,** 648.
Abt, H. A., Morgan, W. W. 1969, *Astr. J.*, **74,** 813.
Anderson, C. M., Stoeckly, R., Kraft, R. P. 1966, *Astrophys. J.*, **143,** 299.
Balona, L. A. 1975, *Mem. R. astr. Soc.*, **78,** 51.
Bidelman, W. P. 1956, *Publ. astr. Soc. Pacific.*, **68,** 318.
Blaauw, A., Hiltner, W. A., Johnson, H. L. 1959, *Astrophys. J.*, **130,** 69; (Erratum) *Astrophys. J.*, **131,** 527.
Braes, L. L. E., 1962, *Bull. astro. Inst. Netherl.*, **16,** 297.
Canterna, R., Perry, C. L., 1979, *Publ. astr. Soc. Pacific*, **91,** 263.
Collins, G. W. II. 1963, *Astrophys. J.*, **138,** 1136.
Collins, G. W. II. 1965, *Astrophys. J.*, **142,** 265.
Collins, G. W. II. 1970, in *IAU Coll. 4: Stellar Rotation*, Ed. A. Slettebak, D. Reidel, Dordrecht, p. 85.
Collins, G. W. II, Harrington, J. P. 1966, *Astrophys. J.*, **146,** 152.
Collins, G. W. II, Smith, R. C. 1985, *Mon. Not. R. astr. Soc.*, **213,** 519.
Collins, G. W. II, Sonneborn, G. H. 1977, *Astrophys. J. Suppl.*, **34,** 41.
Crawford, D. L. 1978, *Astr. J.*, **83,** 48.
Crawford, D. L. 1979, *Astr. J.*, **84,** 1858.
Crawford, D. L., Barnes, J. V. 1969, *Astr. J.*, **74,** 818.
Crawford, D. L., Barnes, J. V. 1969, *Astr. J.*, **74,** 407.
Crawford, D. L., Barnes, J. V. 1970, *Astr. J.*, **75,** 952.
Crawford, D. L., Barnes, J. V. 1972, *Astr. J.*, **77,** 862.
Crawford, D. L., Barnes. J. V. 1974, *Astr. J.*, **79,** 687.
Crawford, D. L., Mander, J. 1966, *Astr. J.*, **71,** 114.
Crawford, D. L., Perry, C. L. 1966, *Astr. J.*, **71,** 206.
Crawford, D. L., Perry, C. L. 1976, *Astr. J.*, **81,** 419.
Dickens, R., Kraft, R., Krzeminski, W. 1968, *Astr. J.*, **73,** 6.
Dworetsky, M. 1975, *Astr. J.*, **80,** 131.
Eggen, O. J. 1974, *Astrophys. J.*, **188,** 59.
Eggen, O. J. 1981, *Astrophys. J.*, **246,** 817.
Feast, M W. 1963, *Mon. Not. R. astr. Soc.*, **126,** 11.
Garmany, C D. 1973, *Astr. J.*, **78,** 185.
Garrison, R. F. 1967, *Astrophys. J.*, **147,** 1003.
Glaspey, J. W. 1971, *Astr. J.*, **76,** 1041.
Gray, R. O., Garrison, R. F. 1987, *Astrophys. J. Suppl.*, **65,** 581.
Gray, R. O., Garrison, R. F. 1989, *Astrophys. J. Suppl.*, **69,** 301.
Gray, R. O., Garrison, R. F. 1989, *Astrophys. J. Suppl.*, **70,** 623.
Guthrie, B. N. G. 1963, *Publ. R. Obs. Edinburgh*, **3,** 84.
Hardorp, J., Strittmatter, P. 1968a, *Astrophys. J.*, **151,** 203.
Hartoog, M. R. 1976, *Astrophys. J.*, **205,** 807.
Hartwick, F. D. A., Hesser, J. E. 1974, *Astrophys. J.*, **192,** 391.

Herzog, A. D., Sanders, W. L., Seggewiss, W. 1975, *Astr. Astrophys. Suppl.*, **19**, 211.
Hill, G., Perry, C. L. 1969, *Astr. J.*, **74**, 1011.
Hoag, A. A., Johnson, H. L., Iriate, B., Hallam, K., Sharpless, S. 1961, *Publ. US Naval Obs.*, **17**, 347.
Hogg, A. R., Kron, G. E. 1955, *Astr. J.*, **60**, 365.
Huang, S. S., Struve, O. 1960, Stellar Atmosphere, Ed. J. L. Greenstein, Univ. Chicago Press, p. 321.
Ianna, P. A. 1970, *Publ. astr. Soc. Pacific*, **82**, 825.
Johnson, H. L. 1952, *Astrophys. J.*, **116**, 640.
Johnson, H. L., Knuckles, C. F. 1955, *Astrophys. J.*, **122**, 209.
Johnson, H. L., Mitchell, R. I. 1958, *Astrophys. J.*, **128**, 31.
Kraft, R. P. 1965, *Astrophys. J.*, **142**, 681.
Kraft, R. P. 1967, *Astrophys. J.*, **148**, 129.
Kraft, R. P. 1969, *Struve Memo. Vol.*, p. 385.
Kraft, R. P., Wrubel, M. 1965, *Astrophys. J.*, **142**, 703.
Levato, H. 1974, *Publ. Astr. Soc. Pacific*, **86**, 940.
Levato, H. 1975, *Astrophys. J.*, **195**, 825.
Levato, H., Garcia, B. 1984, *Astrophys. Lett.*, **24**, 161.
Maeder, A. 1970, *Astr. Astrophys.*, **10**, 354.
Mathew, A., Rajamohan, R. 1990a, *J. Astrophys. Astr.*, **11**, 167 (Paper 2).
Mathew, A., Rajamohan, R. 1990b, *Bull. astr. Soc. India*, **18**, 329.
Mc Gee, J. D., Khogali, A., Baum, W. A., Kraft, R. P. 1967, *Mon. Not. R. astr. Soc.*, **137**, 303.
Mendoza, E. E. 1956, *Astrophys. J.*, **123**, 54.
Mendoza, E. E. 1963, *Bol. Obs. Tonantzintla Tacubaya*, **3**, 137.
Mitchell, R. I. 1960, *Astrophys. J.*, **132**, 68.
Moreno, A., Moreno, H. 1968, *Astrophys. J. Suppl.*, **15**, 459.
Morgan, W. W., Hiltner, W. A. 1965, *Astrophys. J. Suppl.*, **141**, 177.
Morgan, W. W., Hiltner, W. A., Garrison, R. F. 1971, *Astr. J.* **76**, 242.
Nissen, P. E. 1988, *Astr. Astrophys.*, **199**, 146.
Perry, C. L., Bond, H. E. 1969, *Publ. astr. Soc. Pacific*, **81**, 629.
Perry, C. L., Franklin, C. B. Jr., Landolt. A. U., Crawford, D. L. 1976, *Astr. J.*, **81**, 632.
Perry, C. L., Hill, G. 1969, *Astr. J.*, **74**, 899.
Petrie, R. M. 1964, *Publ. Dom. Astrophys. Obs.*, **12**, 317.
Plavec, M. 1970, in *IAU Coll. 4: Stellar Rotation*, Ed. A. Slettebak, D. Reidel, Dordrecht, p. 133.
Rajamohan, R. 1976, *Pramana*, **7**, 160.
Rajamohan, R. 1978, *Mon. Not. R. astr. Soc.*, **184**, 743.
Rajamohan, R., Mathew, A. 1988, *J. Astrophys. Astr.*, **9**, 107.
Roxburgh, I. W. 1970, in *IAU Coll. 4: Stellar Rotation*, Ed. A. Slettebak, D. Reidel, Dordrecht, p. 318.
Roxburgh, I. W., Griffith, J., Sweet, P. 1965, *Z. Astrophys.*, **61**, 203.
Roxburgh, I. W., Strittmatter, P. A. 1965, *Z. Astrophys.*, **63**, 15.
Schild, R. E. 1970, *Astrophys. J.*, **161**, 855.
Schmidt, E. G. 1978, *Pub. astr. Soc. Pacific.*, **90**, 157.
Schmidt, E. G., Forbes, D. 1984, *Mon. Not. R. Astr. Soc.*, **208**, 83.
Shobbrook, R. R. 1984, *Mon. Not. R. astr. Soc.*, **206**, 273.
Shobbrook, R. R. 1984, *Mon. Not. R. astr. Soc.*, **211**, 659.
Slettebak, A. 1968, *Astrophys. J.*, **151**, 1043.
Slettebak, A. 1970, in *IAU Coll. 4:* Stellar Rotation, Ed. A. Slettebak, D. Reidel, Dordrecht, p. 3.
Smyth, M. J., Nandy, K. 1962, *Publ. R. Obs., Edinburgh*, **3**, No. 2, 23.
Snowden, M. S. 1975, *Publ. astr. Soc. Pacific*, **87**, 721.
Snowden, M. S. 1976, *Publ. astr. Soc. Pacific*, **88**, 174.
Strittmatter, P. A. 1966, *Astrophys. J.*, **144**, 430.
Strom, K. M., Strom, S. E., Yost, J. 1971, *Astrophys. J.*, **165**, 479.
Strömgren, B. 1966, *A. Rev. Astr. Astrophys.*, **4**, 433.
Strömgren, B. 1967, *Magnetic and Related Stars*, Ed. R. C. Cameron, Mono Book Corporation, Baltimore, p. 461.
Uesugi, A., Fukuda, I. 1982, *Revised Catalogue of Stellar Rotational Velocities*, Univ. Japan.
Vogel, S. N., Kuhi, L. V. 1981, *Astrophys. J.*, **245**, 960.
Warren, W. H. 1976, *Mon. Not. R. astr. Soc.*, **174**, 111.
Young, A. 1978, *Publ. astr. Soc. Pacific*, **90**, 144.